Thermochemistry and Thermal Decomposition of the Chlorinated Disilanes ($Si_2H_nCl_{6-n}$, $n = 0-6$) Studied by ab Initio Molecular Orbital Methods

Mark T. Swihart* and Robert W. Carr

Department of Chemical Engineering and Materials Science, University of Minnesota, 421 Washington Avenue SE, Minneapolis, Minnesota 55455

Received: May 16, 1997; In Final Form: July 2, 1997[⊗]

The thermochemistry and thermal unimolecular decomposition reactions of the chlorinated disilanes have been characterized using ab initio molecular orbital techniques. Silylene, chlorosilylene, dichlorosilylene, and hydrogen elimination reactions and their reverse insertions were considered. Reactant, product, and transition-state geometries and vibrational frequencies were calculated at the MP2/6-31G(d,p) level. Energetics were obtained at the MP2/6-31+G(2df,p), MP4/6-31+G(2df,p), G2(MP2), and/or G2 levels of theory, depending on the number of chlorine atoms in the molecule. In addition to the expected insertion reactions, direct reaction paths for $SiHCl + SiH_nCl_{4-n} \rightleftharpoons SiH_2 + SiH_{n-1}Cl_{5-n}$ and $SiHCl + SiH_nCl_{4-n} \rightleftharpoons SiCl_2 + SiH_{n+1}Cl_{3-n}$ were observed, with energetic barriers lying a few kcal/mol above the insertion reactions. To our knowledge, these concerted, two-atom exchange reactions have not previously been observed or predicted. They appear to represent a new type of elementary reaction for these compounds. Heats of formation for the chlorinated disilane reactants and chlorinated silylsilylene products of hydrogen elimination were calculated using isodesmic reactions. Energy barriers and conventional transition state theory rate constants for all of the reactions are presented. These can provide a basis for the construction of a detailed mechanism for the multistep thermal decomposition of the chlorinated silanes, which plays an important role in the chemical vapor deposition of epitaxial silicon from the chlorinated silanes.

Introduction

The chlorinated silanes, particularly dichlorosilane and trichlorosilane, are used as precursors for the chemical vapor deposition (CVD) of epitaxial silicon. At the high temperatures where this process is carried out, homogeneous decomposition of the precursor molecules can play an important role by generating reactive species that lead to film growth. Secondary reactions can both accelerate the decomposition of the precursor and consume reactive intermediates that could otherwise lead to film growth. SiHCl and $SiCl_2$, products of direct decomposition of the chlorinated silanes, can insert into the parent molecules to give chlorinated disilanes, which then decompose very quickly. This makes possible complex secondary chemistry involving the chlorinated disilanes. For example, dichlorosilane could decompose in a silylene- or chlorosilylene-catalyzed cycle such as

$$SiHCl + SiH_2Cl_2 \rightarrow HCl_2SiSiH_2Cl$$

$$HCl_2SiSiH_2Cl \rightarrow SiH_3Cl + SiCl_2$$

$$SiH_3Cl \rightarrow SiHCl + H_2$$

This cycle of reactions, and others like it, provide lower energy paths for dichlorosilane decomposition than the corresponding direct reaction $SiH_2Cl_2 \rightarrow SiCl_2 + H_2$, which has a significant activation barrier. To understand the importance of such reactions and develop detailed kinetic models for the decomposition of chlorinated silanes, we need rates for the thermal decomposition reactions of the chlorinated disilanes and their reverse reactions, the insertion of SiH_2, SiHCl, and $SiCl_2$ into the chlorinated silanes.

Theoretical investigations of the thermochemistry and thermal decomposition of silanes and halosilanes have been reviewed by Gordon et al.[1] The kinetics and mechanisms of silylene reactions have been reviewed by Becerra et al.[2] and Jasinski et al.[3] Elimination of silylene from disilane and the reverse insertion reaction have been well studied both experimentally[4−9] and theoretically.[4,5,10−13] The insertion reaction is effectively barrierless and exothermic by about 54 kcal/mol. Thermal decomposition reactions of the chlorinated silanes were studied theoretically by Su and Schlegel.[14,15] In this work we use the same levels of calculation and basis sets as those used by Su and Schlegel, so that consistent thermochemical and kinetic parameters can be obtained. Wittbrodt and Schlegel have recently published higher level calculations for dichlorosilane decomposition.[16] These results differed only slightly from the previous study. Hay[17] has recently assessed the use of density functional methods for calculating the thermochemistry of Si−H−Cl compounds and found that while DFT methods were promising, they did not do as well as the high-level conventional methods used here. Ignacio and Schlegel[18] performed calculations similar to those presented here for the fluorinated disilanes with up to two fluorine atoms. McKean et al.[19,20] have calculated structures and vibrational frequencies for the chlorinated disilanes with up to three chlorine atoms in conjunction with an experimental study of the infrared spectra of these compounds, but they did not present calculated energies. To our knowledge, there have been no previously published theoretical studies of either the thermochemistry or reactions of the chlorinated disilanes. There is experimental information for the insertion of SiHCl into SiH_4 and SiH_2Cl_2 at room temperature.[21] The insertion rate was roughly the same for both reactions and indicated that there is a significant barrier to this insertion. Jenkins et al.[22] measured relative rates of SiH_2, SiHCl, and $SiCl_2$ elimination from $H_2ClSiSiH_3$ and HCl_2SiSiH_3. They observed comparable rates for competing elimination reactions.

[⊗] Abstract published in *Advance ACS Abstracts,* September 15, 1997.

Doncaster and Walsh[23] investigated the thermal decomposition of Si_2Cl_6 and found an activation energy of 49 kcal/mol for $SiCl_2$ elimination near 600 K.

Based on our knowledge of disilane decomposition, chlorinated silane decomposition, and estimates of the thermochemistry from the sources cited above, there are four possible reactions for the decomposition of a chlorinated disilane. These are elimination of SiH_2, elimination of SiHCl, elimination of $SiCl_2$, and 1,1 elimination of H_2. Direct cleavage of any of the bonds would be too endothermic to be competitive with these channels, as would elimination of HCl or Cl_2. 1,2-Hydrogen elimination from disilane was found to have a high barrier[11] and be unimportant compared to 1,1-elimination. This is expected to be true for the chlorinated disilanes as well, so the 1,2-elimination is not considered here. Preliminary estimates of the thermochemistry were made by assuming that each chlorine substitution results in a constant increment of the heats of formation. In the decomposition direction, SiH_2 elimination and H_2 elimination are roughly 55 kcal/mol endothermic, SiHCl elimination is roughly 44 kcal/mol endothermic, and $SiCl_2$ elimination is roughly 33 kcal/mol endothermic. However, the order of reactivity of the silylenes is well established as $SiH_2 > SiHCl > SiCl_2$, so we expect the barriers for the reverse reactions to increase from SiH_2, which has no barrier for insertion into silane,[4] to SiHCl, which has a barrier for insertion into silane and dichlorosilane,[21] to $SiCl_2$. The insertion of H_3SiSiH into H_2 has almost no barrier, so we might expect the corresponding insertions of chlorinated silylsilylenes into hydrogen, the reverse of 1,1-hydrogen elimination, to also have small barriers. Thus, these four primary decomposition paths could all be competitive with one another, and we investigate all of them, realizing that different reactions could dominate for the different chlorinated disilanes.

Computational Method

The ab initio molecular orbital calculations presented here were carried out using the GAUSSIAN 94 series of programs.[24] Geometries were fully optimized using the "tight" convergence criteria at the MP2(full)/6-31G(d,p) level using analytical gradients. Vibrational frequencies were obtained at this same level using analytical second derivatives. The frequency calculations verified that the points located were indeed minima or first-order saddle points with zero or one imaginary frequency, respectively. Energies were calculated using a larger basis set and second-order Møller−Plesset perturbation theory (MP2/6-31+G(2df,p), frozen core) for all of the species considered. For molecules and transition states with three or fewer chlorine atoms, energies were also calculated using fourth-order Møller−Plesset theory (MP4SDTQ/6-31+G(2df,p),frozen core) and at the G2(MP2)[25] level. Full G2[26] energy calculations were performed for those molecules with two or fewer chlorines. The G2 methods approximate a quadratic configuration interaction[27] calculation at the QCISD(T)/6-311+G(3df,2p) level by applying basis set corrections additively to a QCISD(T)/6-311G(d,p) calculation.[26] In the original G2 method, some of these corrections are calculated at the MP4 level, whereas in the modified G2(MP2) method, all of the corrections are calculated at the MP2 level.[25] In both cases, zero-point energy based on the HF/6-31G(d) frequencies, scaled by 0.8929, is added to the energy, as is an empirical correction based on the number of paired and unpaired electrons in the molecule. Note that in all of the reactions considered here, all of the electrons remain formally paired, so that this empirical correction in the G2 methods cancels when taking energy differences between reactants and products or transition states.

Results and Discussion

The total energies for reactants, products, and transition states calculated in this work are given in Table 1. The energies of the chlorinated silanes and silylenes at these levels have been previously published by Su and Schlegel.[14] Our calculated results are identical with theirs and are presented here only for convenience. We have added the G2(MP2) calculations for these species and the G2 calculations for $SiHCl_3$ and $SiCl_4$. G2 energies for disilane and silylsilylene have also been previously published.[28] Again, our results are identical. The zero-point energies and thermal energies are calculated from the geometries and unscaled frequencies at the MP2(full)/6-31G(d,p) level in the rigid rotor, harmonic oscillator approximations.

Geometries and Frequencies. Generic representations of a chlorinated silylsilylene and a chlorinated disilane are presented in Figure 1, parts a and b, respectively. The atoms numbered 1 and 2 are silicon for all of the structures considered, whereas those numbered 3 and higher can be either chlorine or hydrogen. The geometric parameters for these structures are given in Table 2. The atom labeling in Table 2 corresponds to the numbering in Figure 1. The geometries are described by bond lengths, bond angles, all relative to the Si−Si bond, and dihedral angles about the Si−Si bond, relative to the atom numbered 3 in the figure. In all cases, the structure given is that believed to be the lowest energy rotamer, although the other rotamers may be very close in energy to the one shown. There is little change in the geometries with chlorine substitution.

Figure 2 gives generic representations of the four types of transition-state structures considered here. The geometric parameters for these structures are presented in Table 3 and are the same bond lengths and angles used to describe the chlorinated disilanes. Figure 2a is the transition state for elimination of SiH_2, SiHCl, or $SiCl_2$. The atoms numbered 3−8 can be either hydrogen or chlorine. For some reactions there are multiple rotamers of this structure, obtained by interchanging atoms 3, 4, and 5. In those cases, only the structure believed to be the lowest energy rotamer is given. Note that there are some reactions where the transition state has C_s symmetry. However, there are others where C_s symmetry would be possible, including SiH_2 elimination from H_3SiSiH_3 and $SiCl_2$ elimination from HCl_2SiSiH_3, that have transition states which distort to C_1 symmetry. There is little change in the geometry of these structures with chlorine substitution. The Si−Si distance in the transition state tends to be longest for SiH_2 elimination and shortest for $SiCl_2$ elimination. This can be explained by the fact that the reaction endothermicity increases from $SiCl_2$ to SiHCl to SiH_2, while the height of the barrier to reaction changes very little. This would lead us to expect that the transition-state location would move closer to the products as we go from $SiCl_2$ to SiHCl to SiH_2, and this is what is observed. It is expected that for each of the structures such as Figure 2a, there is a corresponding potential minimum with similar geometry but with the inserting chlorinated silylene further removed from the chlorinated silane. These clusters are known to exist for SiH_2 insertion into SiH_4[4] and for SiH_2, SiHCl, and $SiCl_2$ insertions into H_2, HCl, and Cl_2.[15] We located such clusters for the insertions of SiHCl into SiH_4 and SiH_2 into SiH_3Cl, but to conserve limited computational resources did not characterize them with higher level energy calculations. We did not attempt to locate the clusters for reactions with more than one chlorine.

Figure 2b shows the generic geometry for H_2 elimination. Atoms 3−6 can be hydrogen or chlorine, but atoms 7 and 8 are always hydrogen. Again, only the lowest energy rotamer is given. The transition-state geometry is almost unaffected by

TABLE 1: Total Energies[a]

	MP2 6-31G(d,p)	MP2 6-31+G(2df,p)	MP4 6-31+G(2df,p)	G2(MP2)	G2	ZPE	thermal + ZPE
Stable Molecules							
H_2	−1.157 66	−1.157 66	−1.164 56	−1.166 36	−1.166 36	6.589	8.070
HCl	−460.215 62	−460.257 26	−460.284 61	−460.331 62	−460.340 17	4.471	5.952
Cl_2	−919.191 22	−919.284 23	−919.334 12	−919.425 73	−919.442 21	0.781	2.383
SiH_2	−290.093 98	−290.106 22	−290.134 49	−290.164 26	−290.167 71	7.763	9.558
SiHCl	−749.195 37	−749.255 01	−749.300 33	−749.375 27	−749.385 96	5.098	7.036
$SiCl_2$	−1208.301 79	−1208.409 87	−1208.472 01	−1208.592 40	−1208.610 39	1.842	4.210
SiH_4	−291.349 86	−291.364 78	−291.396 56	−291.415 55	−291.419 07	20.565	22.462
SiH_3Cl	−750.434 14	−750.496 47	−750.545 32	−750.610 44	−750.621 81	17.307	19.408
SiH_2Cl_2	−1209.520 71	−1209.630 82	−1209.696 86	−1209.808 94	−1209.828 18	13.536	16.092
$SiHCl_3$	−1668.607 26	−1668.765 26	−1668.848 59	−1669.008 35	−1669.035 48	9.313	12.529
$SiCl_4$	−2127.691 64	−2127.897 26	−2127.997 99	−2128.206 00	−2128.241 13	4.809	8.794
H3SiSiH	−580.280 05	−580.308 69	−580.361 81	−580.410 77	−580.417 83	20.161	23.087
$H_3SiSiCl$	−1039.378 02	−1039.455 17	−1039.525 29	−1039.620 09	−1039.634 33	17.024	20.429
$H_2ClSiSiH$	−1039.365 67	−1039.441 96	−1039.512 03	−1039.607 87	−1039.622 54	16.582	19.915
$H_2ClSiSiCl$	−1498.463 66	−1498.588 52	−1498.675 58	−1498.817 56	−1498.839 37	13.387	17.328
HCl_2SiSiH	−1498.454 22	−1498.579 31	−1498.666 04	−1498.809 38	−1498.831 50	12.877	16.822
$HCl_2SiSiCl$	−1957.551 62	−1957.724 47	−1957.828 47	−1958.018 08		9.477	14.112
Cl_3SiSiH	−1957.543 67	−1957.715 13	−1957.819 12	−1958.010 25		8.529	13.308
$Cl_3SiSiCl$	−2416.640 66	−2416.860 96				5.165	10.600
H_3SiSiH_3	−581.534 62	−581.564 54	−581.621 23	−581.660 95	−581.668 09	32.245	35.314
$H_2ClSiSiH_3$	−1040.618 61	−1040.696 08	−1040.769 76	−1040.856 25	−1040.871 16	28.629	32.188
HCl_2SiSiH_3	−1499.706 11	−1499.831 29	−1499.922 00	−1500.055 98	−1500.078 68	24.613	28.839
$H_2ClSiSiH_2Cl$	−1499.702 51	−1499.827 57	−1499.918 26	−1500.051 81	−1500.074 50	24.943	29.073
HCl_2SiSiH_2Cl	−1958.789 19	−1958.962 22	−1959.069 99	−1959.251 26		20.884	25.697
Cl_3SiSiH_3	−1958.795 11	−1958.967 73	−1959.075 52	−1959.257 66		20.289	25.286
$HCl_2SiSiHCl_2$	−2417.875 77	−2418.096 92				16.765	22.305
Cl_3SiSiH_2Cl	−2417.877 76	−2418.098 32				16.560	22.148
$Cl_3SiSiHCl_2$	−2876.964 23	−2877.232 89				12.454	18.761
$Cl_3SiSiCl_3$	−3336.052 76	−3336.368 86				8.095	15.199
Transition States with Structure of Figure 2a							
$H_3SiSiH_3 \leftrightarrow SiH_4 + SiH_2$	−581.454 40	−581.489 51	−581.547 61	−581.590 53	−581.597 04	31.196	33.995
$H_2ClSiSiH_3 \leftrightarrow SiH_3Cl + SiH_2$[b]	−1040.535 82	−1040.617 68	−1040.693 57	−1040.784 38	−1040.798 70	27.693	31.033
$H_2ClSiSiH_3 \leftrightarrow SiH_3Cl + SiH_2$[c]	−1040.524 54	−1040.611 74	−1040.686 15	−1040.775 20	−1040.789 53	27.728	31.057
$H_2ClSiSiH_3 \leftrightarrow SiH_4 + SiHCl$	−1040.534 76	−1040.617 84	−1040.693 09	−1040.783 30	−1040.797 31	27.632	30.917
$H_2ClSiSiH_2Cl \leftrightarrow SiH_2Cl_2 + SiH_2$	−1499.617 37	−1499.753 08	−1499.844 16	−1499.980 03	−1500.002 20	23.899	27.775
$H_2ClSiSiH_2Cl \leftrightarrow SiH_3Cl + SiHCl$	−1499.624 42	−1499.755 17	−1499.847 12	−1499.984 36	−1500.006 28	23.866	27.647
$HCl_2SiSiH_3 \leftrightarrow SiH_2Cl_2 + SiH_2$	−1499.619 19	−1499.749 41	−1499.842 51	−1499.981 40	−1500.003 46	23.489	27.512
$HCl_2SiSiH_3 \leftrightarrow SiH_3Cl + SiHCl$	−1499.614 76	−1499.750 34	−1499.841 77	−1499.977 74	−1499.999 65	23.975	27.972
$HCl_2SiSiH_3 \leftrightarrow SiH_4 + SiCl_2$	−1499.613 54	−1499.744 47	−1499.837 06	−1499.975 09	−1499.996 73	23.734	27.638
$HCl_2SiSiH_2Cl \leftrightarrow SiHCl_3 + SiH_2$	−1958.697 73	−1958.881 93	−1958.990 66	−1959.175 07		19.477	24.113
$HCl_2SiSiH_2Cl \leftrightarrow SiH_2Cl_2 + SiHCl$[b]	−1958.706 93	−1958.886 40	−1958.995 57	−1959.180 42		19.761	24.276
$HCl_2SiSiH_2Cl \leftrightarrow SiH_2Cl_2 + SiHCl$[c]	−1958.705 78	−1958.889 97	−1958.998 02	−1959.181 17		20.052	24.626
$HCl_2SiSiH_2Cl \leftrightarrow SiH_3Cl + SiCl_2$	−1958.703 66	−1958.882 31	−1958.991 56	−1959.176 90		19.868	24.329
$Cl_3SiSiH_3 \leftrightarrow SiHCl_3 + SiH_2$	−1958.705 17	−1958.882 81	−1958.993 25	−1959.180 27		19.124	23.914
$Cl_3SiSiH_3 \leftrightarrow SiH_3Cl + SiCl_2$	−1958.706 86	−1958.890 69	−1958.999 12	−1959.182 76		19.851	24.647
$HCl_2SiSiHCl_2 \leftrightarrow SiHCl_3 + SiHCl$	−2417.788 11	−2418.020 74				15.698	21.037
$HCl_2SiSiHCl_2 \leftrightarrow SiH_2Cl_2 + SiCl_2$	−2417.786 94	−2418.013 90				15.864	21.027
$Cl_3SiSiH_2Cl \leftrightarrow SiCl_4 + SiH_2$	−2417.777 13	−2418.009 12				14.930	20.378
$Cl_3SiSiH_2Cl \leftrightarrow SiHCl_3 + SiHCl$	−2417.790 73	−2418.018 11				15.455	20.747
$Cl_3SiSiH_2Cl \leftrightarrow SiH_2Cl_2 + SiCl_2$	−2417.795 59	−2418.027 85				15.882	21.255
$Cl_3SiSiHCl_2 \leftrightarrow SiCl_4 + SiHCl$	−2876.868 88	−2877.149 21				11.153	17.317
$Cl_3SiSiHCl_2 \leftrightarrow SiHCl_3 + SiCl_2$[b]	−2876.870 11	−2877.145 53				11.357	17.348
$Cl_3SiSiHCl_2 \leftrightarrow SiHCl_3 + SiCl_2$[c]	−2876.880 58	−2877.159 90				11.821	18.003
$Cl_3SiSiCl_3 \leftrightarrow SiCl_4 + SiCl_2$	−3335.962 19	−3336.291 02				7.187	14.110
Transition States with Structure of Figure 2b							
$H_3SiSiH_3 \leftrightarrow H_3SiSiH + H_2$	−581.440 97	−581.475 63	−581.532 94	−581.578 69	−581.585 04	29.919	32.925
$H_2ClSiSiH_3 \leftrightarrow H_3SiSiCl + H_2$	−1040.520 68	−1040.604 87	−1040.678 99	−1040.771 49	−1040.785 04	26.220	29.754
$H_2ClSiSiH_3 \leftrightarrow H_2ClSiSiH + H_2$	−1040.526 29	−1040.609 20	−1040.683 35	−1040.775 96	−1040.790 00	26.164	29.697
$H_2ClSiSiH_2Cl \leftrightarrow H_2ClSiSiCl + H_2$	−1499.605 73	−1499.738 06	−1499.828 98	−1499.968 52	−1499.989 84	22.527	26.608
$HCl_2SiSiH_3 \leftrightarrow HCl_2SiSiH + H_2$	−1499.614 25	−1499.745 24	−1499.836 26	−1499.976 57	−1499.998 26	22.121	26.317
$HCl_2SiSiH_2Cl \leftrightarrow HCl_2SiSiCl + H_2$	−1958.692 61	−1958.873 11	−1958.980 94	−1959.168 67		18.318	23.138
$Cl_3SiSiH_3 \leftrightarrow Cl_3SiSiH + H_2$	−1958.702 42	−1958.880 62	−1958.988 74	−1959.177 31		17.782	22.730
$Cl_3SiSiH_2Cl \leftrightarrow Cl_3SiSiCl + H_2$	−2417.780 08	−2418.008 40				14.028	19.596
Transition States with Structure of Figure 2c							
$SiH_4 + SiHCl \leftrightarrow SiH_3Cl + SiH_2$	−1040.509 58	−1040.597 82	−1040.673 12	−1040.763 69	−1040.777 38	28.071	31.279
$SiH_3Cl + SiHCl \leftrightarrow SiH_2Cl_2 + SiH_2$	−1499.599 87	−1499.735 72	−1499.828 02	−1499.965 43	−1499.986 86	24.547	28.191
$SiH_3Cl + SiHCl \leftrightarrow SiH_4 + SiCl_2$	−1499.604 33	−1499.741 78	−1499.833 99	−1499.971 62	−1499.992 62	24.072	28.054
$SiH_2Cl_2 + SiHCl \leftrightarrow SiHCl_3 + SiH_2$	−1958.686 48	−1958.871 41	−1958.980 80	−1959.165 17		20.406	24.777
$SiH_2Cl_2 + SiHCl \leftrightarrow SiH_3Cl + SiCl_2$	−1958.694 88	−1958.879 63	−1958.988 90	−1959.173 67		20.490	24.928
$SiHCl_3 + SiHCl \leftrightarrow SiCl_4 + SiH_2$	−2417.766 13	−2418.000 84				15.935	20.976
$SiHCl_3 + SiHCl \leftrightarrow SiH_2Cl_2 + SiCl_2$	−2417.780 94	−2418.014 18				16.196	21.466
$SiCl_4 + SiHCl \leftrightarrow SiHCl_3 + SiCl_2$	−2876.858 91	−2877.141 64				11.594	17.622

TABLE 1 (Continued)

	MP2 6-31G(d,p)	MP2 6-31+G(2df,p)	MP4 6-31+G(2df,p)	G2(MP2)	G2	ZPE	thermal + ZPE
			Transition States with Structure of Figure 2d				
$H_3SiSiH_3 \leftrightarrow SiH_4 + SiH_2$	−581.456 76	−581.491 38	−581.549 63	−581.593 66	−581.599 77	31.485	34.329
$H_2ClSiSiH_3 \leftrightarrow SiH_3Cl + SiH_2$	−1040.537 90	−1040.619 44	−1040.695 23	−1040.786 60	−1040.800 66	27.827	31.109

[a] Total energies in hartrees (1 hartree = 627.51 kcal/mol), zero-point energies (ZPE), and thermal energy in kcal/mol at 298 K and 1 atm using geometry and unscaled frequencies at the MP2/6-31G(d,p) level. MP2/6-31+G(2df,p) and MP4/6-31+G(2df,p) energies are at MP2/6-31G(d,p) geometry. Note that G2 and G2(MP2) energies include zero-point energy calculated using scaled HF/6-31G(d) frequencies. Entries left blank were not calculated due to computational expense. [b] Transition state corresponding to insertion into Si−H bond. [c] Transition state corresponding to insertion into Si−Cl bond.

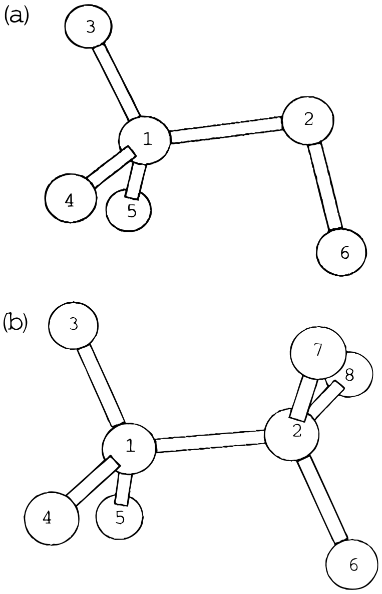

Figure 1. Generic molecular geometries. Atoms 1 and 2 are silicon: atoms 3−8 may be hydrogen or chlorine. Bond lengths and angles are given in Table 2.

chlorine substitution. Potential minima with the H_2 molecule further removed from the chlorinated silylsilylene are expected to be present for these reactions, analogous to those for insertion of SiH_2, SiHCl, and $SiCl_2$ into H_2.[15] These were located for $H_3SiSiCl$ and $H_2ClSiSiH$ insertions into H_2. We did not attempt to locate them for the reactions where more than one chlorine atom is present.

Figure 2d shows an alternative geometry for the elimination and insertion of SiH_2. For SiH_2 insertion into SiH_4, this type of geometry has been presented and discussed by several authors.[4,5,12] It lies approximately 8 kcal/mol below the separated SiH_2 and SiH_4. We found that following the minimum energy path from this point toward $SiH_4 + SiH_2$ (at the MP2/6-31G(d,p) level) leads to a potential minimum of similar geometry but with SiH_2 further removed from SiH_4. This cluster can presumably form from SiH_2 and SiH_4 with no barrier. Following the minimum energy path toward disilane leads to another minimum in energy which has C_{3v} symmetry and corresponds to a complex between a normal SiH_3 group and an inverted SiH_3 group. This is the structure presented by Becerra et al.,[4] who showed that it can convert to disilane with a very small barrier. Thus, it appears that the insertion of SiH_2 into SiH_4 proceeding along this path would go first through a structure like that of Figure 2d, then through the C_{3v} structure and on to disilane. It should be kept in mind that the potential surface in this region is quite flat and the barriers are small, so that the insertion is not tightly constrained to this path, and there may be completely barrierless paths that have not been discovered. With this in mind, we located transition states with structures such as Figure 2d for insertion of SiH_2 into the Si−H bonds of SiH_4 and SiH_3Cl. We were unable to locate corresponding structures for insertion of SiH_2 into the Si−H bonds of SiH_2Cl_2 and $SiHCl_3$. In these cases the potential surface is still very flat near the expected geometry for this structure, but appears not to have a saddle point.

Attempts to locate a structure like that of Figure 2d for insertions of SiHCl and $SiCl_2$ into Si−H and Si−Cl bonds and for insertions of SiH_2 into Si−Cl bonds led instead to the structure shown in Figure 2c. In this structure, atom 6 is chlorine and atom 7 is hydrogen. Reaction paths passing through this transition state do not lead to insertion, but instead lead to the concerted four-centered exchange of a hydrogen atom for a chlorine atom between the two silicon centers. This exchange motion is shown clearly when one looks at the normal mode corresponding to the imaginary vibrational frequency of this structure. For the reaction

$$SiHCl + SiH_4 \rightleftharpoons SiH_2 + SiH_3Cl$$

we followed the minimum energy path at the HF/6-31G(d) level from the structure of Figure 2c in both directions. This path connected to a cluster of SiHCl and SiH_4 in one direction and a cluster of SiH_2 and SiH_3Cl in the other, confirming the path of this exchange reaction through the transition structure of Figure 2c. To our knowledge, these concerted, two-atom exchange reactions have not previously been observed or predicted for these compounds. Geometric parameters for the transition states for the eight possible reactions of this type are given in Table 3. Only the lowest energy rotamer of each structure is given. Based on the Si−H and Si−Cl distances, these appear to be genuinely four-centered structures. Both the hydrogen atom (7) and the chlorine atom (6) are approximately equidistant from the two silicon atoms in this structure. The distances $R(2-6)$ and $R(2-7)$ are given in Table 3 and range from 2.29 to 2.35 Å and 1.58 to 1.66 Å, respectively. The corresponding distances to the other silicon atom, $R(1-6)$ and $R(1-7)$, range from 2.28 to 2.41 Å and 1.60 to 1.73 Å, respectively. For all of the structures of type 2c the difference between the two Si−Cl distances is 0.12 Å or less, and the difference between the two Si−H distances is 0.14 Å or less.

Computed vibrational frequencies for the chlorinated disilanes, chlorinated silylsilylenes, and transition states are given in Table 4. There is limited experimental information on these compounds that can be used to estimate a scaling factor for the frequencies. Matching the calculated frequencies to experimental anharmonic frequencies for disilane[29] requires a mean scaling factor of 0.938. The Si−H stretching frequencies of $H_2ClSiSiH_3$, $H_2ClSiSiH_2Cl$, HCl_2SiSiH_3, and HCl_2SiSiH_2Cl would require scaling by a factor of 0.928 to match those measured by McKean et al.[19,20] Schlegel[14] suggested a scaling factor of 0.945 for the frequencies of SiH_mCl_n calculated at the same level, for which a number of comparisons with experimental frequencies were possible. Thus it appears that a factor of 0.93−0.94 is probably appropriate.

TABLE 2: Parameters of MP2/6-31G(d,p) Optimized Molecular Geometries[a]

molecules with structure of Figure 1a	atom labels	symmetry	R(1−2)	R(1−3)	R(1−4)	R(1−5)	R(2−6)	∠213	∠214	∠215	∠126	∠4123	∠5123	∠6213
H_3SiSiH	SiSiH H H H	C_s	2.381	1.477	1.481	1.481	1.510	114.2	109.4	109.4	89.3	−121.0	121.0	180.0
$H_3SiSiCl$	SiSiH H H Cl	C_s	2.402	1.479	1.479	1.479	2.089	111.8	109.5	109.5	95.4	−120.4	120.4	180.0
$H_2ClSiSiH$	SiSiClH H H	C_s	2.372	2.073	1.478	1.478	1.514	113.7	110.3	110.3	86.6	−120.2	120.2	180.0
$H_2ClSiSiCl$	SiSiClH H Cl	C_s	2.401	2.072	1.476	1.476	2.090	110.7	110.7	110.7	93.0	−119.6	119.6	180.0
HCl_2SiSiH	SiSiClH ClH	C_1	2.359	2.057	1.471	2.081	1.511	116.1	123.4	93.4	87.8	−133.4	113.9	161.4
$HCl_2SiSiCl$	SiSiClH ClCl	C_1	2.401	2.060	1.472	2.066	2.082	110.3	118.6	103.8	95.1	−124.1	117.3	144.7
Cl_3SiSiH	SiSiClClClH	C_s	2.377	2.052	2.056	2.506	1.507	114.2	109.7	109.7	86.9	−120.2	120.2	180.0
$Cl_3SiSiCl$	SiSiClClClCl	C_s	2.413	2.054	2.051	2.051	2.071	109.7	111.3	111.3	95.5	−119.3	119.3	180.0

molecules with structure of Figure 1b	atom labels	symmetry	R(1−2)	R(1−3)	R(1−4)	R(1−5)	R(2−6)	R(2−7)	R(2−8)	∠213	∠214	∠215	∠126	∠127	∠128	∠4123	∠5123	∠6213	∠7213	∠8213
H_3SiSiH_3	SiSiH H H H H H	D_{3d}	2.334	1.476	1.476	1.476	1.476	1.476	1.476	110.4	110.4	110.4	110.4	110.4	110.4	−120.0	120.0	180.0	60.0	−60.0
$H_2ClSiSiH_3$	SiSiClH H H H H	C_s	2.332	2.069	1.473	1.473	1.477	1.474	1.474	109.3	111.6	111.6	109.4	109.7	109.7	−119.1	119.1	180.0	60.1	−60.1
HCl_2SiSiH_3	SiSiH ClClH H H	C_s	2.329	1.470	2.057	2.057	1.473	1.474	1.474	114.7	109.4	109.4	108.4	109.2	109.2	−120.0	120.0	180.0	60.1	−60.1
$H_2ClSiSiH_2Cl$	SiSiClH H ClH H	C_{2h}	2.331	2.067	1.472	1.472	2.067	1.472	1.472	108.1	111.1	111.1	108.1	111.1	111.1	−118.9	118.9	180.0	61.1	−61.1
HCl_2SiSiH_2Cl	SiSiH ClClH H Cl	C_1	2.330	1.469	2.055	2.050	1.471	1.472	2.060	114.0	107.7	109.7	109.7	110.0	108.9	−119.5	120.8	−175.1	63.4	−55.7
Cl_3SiSiH_3	SiSiClClClH H H	C_{3v}	2.325	2.048	2.048	2.048	1.473	1.473	1.473	110.7	110.7	110.7	108.4	108.4	108.4	−120.0	120.0	180.0	60.0	−60.0
$HCl_2SiSiHCl_2$	SiSiH ClClH ClCl	C_{2h}	2.331	1.468	2.049	2.049	1.468	2.049	2.049	112.6	108.6	108.6	112.6	108.6	108.6	−120.1	120.1	180.0	59.9	−59.9
Cl_3SiSiH_2Cl	SiSiClClClClH H	C_s	2.327	2.047	2.042	2.042	2.054	1.471	1.471	108.6	110.9	110.9	109.0	109.1	109.1	−119.5	119.5	180.0	60.6	−60.6
$Cl_3SiSiHCl_2$	SiSiClClClH ClCl	C_s	2.327	2.036	2.041	2.041	1.468	2.043	2.043	110.3	109.3	109.3	111.4	108.6	108.6	−120.3	120.3	180.0	60.2	−60.2
$Cl_3SiSiCl_3$	SiSiClClClClClCl	D_{3d}	2.324	2.036	2.036	2.036	2.036	2.036	2.036	109.3	109.3	109.3	109.3	109.3	109.3	−120.0	120.0	180.0	60.0	−60.0

[a] Bond lengths in angstroms; bond angles and dihedral angles in degrees. Atom numbering as shown in Figure 1, i.e., SiSiH ClH H H Cl means the atoms labeled 1 and 2 are Si, atoms 3, 5, 6, and 7 are H, and atoms 4 and 8 are Cl in Figure 1b.

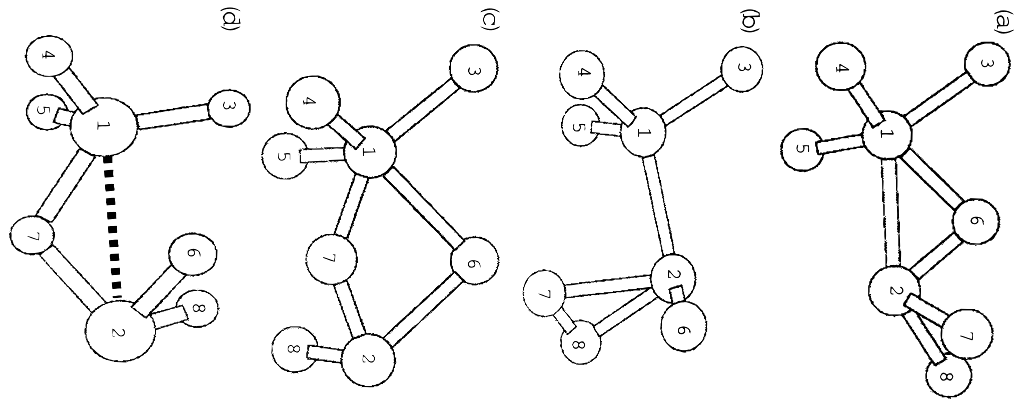

Figure 2. Generic geometries for the four types of transition states considered in this paper. Atoms 1 and 2 are silicon: atoms 3−8 may be hydrogen or chlorine. Bond lengths and angles are given in Table 3.

Heats of Formation. Heats of formation for the chlorinated disilanes and chlorinated silylsilylenes were calculated from the energies given in Table 1 and are presented in Table 5. The heats of formation of the chlorinated disilanes were calculated using the isodesmic reaction

$$Si_2H_6 + \frac{n}{4}\,SiCl_4 \rightarrow Si_2H_{6-n}Cl_n + \frac{n}{4}\,SiH_4$$

For the chlorinated silylsilylenes, the reaction

$$SiH_2 + Si_2H_6 + \frac{n}{4}\,SiCl_4 \rightarrow Si_2H_{4-n}Cl_n + \left(1 + \frac{n}{4}\right) SiH_4$$

was used to compute the heats of formation. Experimental heats of formation for SiH_4,[30] $SiCl_4$,[30] Si_2H_6,[31] and SiH_2[4] were used as references. For the results in Table 5, there is very good agreement among all of the levels of theory used, including MP2/6-31G(d,p). This increases our confidence in the results for the more chlorinated species for which MP2/6-31+G(2df,p) calculations were the highest level that could be performed. The heats of formation of SiH_4 and $SiCl_4$ are well established and show good agreement between experiment and theory. The heat of formation used for Si_2H_6 (19.1 kcal/mol) is from the CATCH tables.[31] This differs somewhat from the best theoretical estimates for Si_2H_6,[28] which predict a heat of formation of 16 kcal/mol. However, the $\Delta H_f°$ of SiH_2 used as a reference here

TABLE 3: Parameters of MP2/6-31G(d,p) Optimized Transition State Geometries[a]

	atom labels	symmetry	R(1−2)	R(1−3)	R(1−4)	R(1−5)	R(2−6)	R(2−7)	R(2−8)	∠213	∠214	∠215	∠126	∠127	∠128	∠4123	∠5123	∠6213	∠7213	∠8213
Transition States with Structure of Figure 2a																				
$H_3SiSiH_3 \leftrightarrow SiH_4+SiH_2$	SiSiH H H H H H	C_s	2.457	1.482	1.469	1.469	1.671	1.489	1.489	130.6	98.6	98.6	41.4	107.8	107.8	−121.3	121.3	0.0	55.1	−55.1
$H_2ClSiSiH_3 \leftrightarrow SiH_3Cl+SiH_2$[b]	SiSiH ClH H H H	C_1	2.754	1.469	2.036	1.461	1.782	1.502	1.505	134.6	101.8	87.0	30.6	103.4	92.2	−130.0	117.0	19.3	47.7	−49.1
$H_2ClSiSiH_3 \leftrightarrow SiH_3Cl+SiH_2$[c]	SiSiH H H ClH H	C_s	2.624	1.482	1.468	1.468	2.350	1.488	1.488	148.1	91.2	91.2	52.9	124.6	124.6	−121.3	121.3	0.0	70.4	−70.4
$H_2ClSiSiH_3 \leftrightarrow SiH_4+SiHCl$	SiSiH H H H ClH	C_1	2.321	1.485	1.504	1.478	1.598	2.081	1.520	117.6	111.1	100.5	54.7	116.4	120.3	−122.8	120.6	−34.0	46.4	−90.0
$H_2ClSiSiH_2Cl \leftrightarrow SiH_2Cl_2+SiH_2$	SiSiClH H ClH H	C_s	2.552	2.099	1.462	1.462	2.336	1.484	1.484	154.1	91.3	91.3	53.1	124.2	124.2	−118.2	118.2	0.0	71.7	−71.7
$H_2ClSiSiH_2Cl \leftrightarrow SiH_3Cl+SiHCl$	SiSiClH H H ClH	C_1	2.336	2.077	1.466	1.466	1.652	2.069	1.477	130.1	103.6	97.0	46.7	118.2	115.1	−119.5	119.9	−16.4	56.8	−72.0
$HCl_2SiSiH_3 \leftrightarrow SiH_2Cl_2+SiH_2$	SiSiH ClClH H H	C_s	2.814	1.464	2.026	2.026	1.794	1.503	1.503	135.7	95.5	95.5	28.8	97.4	97.4	−122.5	122.5	0.0	48.4	−48.4
$HCl_2SiSiH_3 \leftrightarrow SiH_3Cl+SiHCl$	SiSiH H H ClClH	C_1	2.582	1.479	1.470	1.470	2.348	2.072	1.485	146.8	90.9	92.4	54.5	122.8	129.0	−120.8	122.2	−0.4	82.8	−65.9
$HCl_2SiSiH_3 \leftrightarrow SiH_4+SiCl_2$	SiSiH H H H ClCl	C_1	2.378	1.477	1.474	1.467	1.658	2.071	2.070	125.3	103.7	97.1	46.0	117.6	116.7	−120.8	123.5	−29.0	36.5	−94.7
$HCl_2SiSiH_2Cl \leftrightarrow SiHCl_3+SiH_2$	SiSiClClH ClH H	C_1	2.701	2.074	2.040	1.456	2.421	1.488	1.489	156.2	92.2	86.6	48.9	121.4	122.2	−128.4	111.9	10.6	76.8	−54.2
$HCl_2SiSiH_2Cl \leftrightarrow SiH_2Cl_2+SiHCl$[b]	SiSiClH ClH ClH	C_1	2.375	2.061	1.463	2.038	1.684	2.074	1.480	129.6	102.2	100.6	44.0	113.7	112.2	−117.4	125.3	−26.2	46.3	−74.8
$HCl_2SiSiH_2Cl \leftrightarrow SiH_2Cl_2+SiHCl$[c]	SiSiClH H ClClH	C_1	2.484	2.096	1.465	1.465	2.310	2.060	1.480	151.4	92.3	93.7	56.1	123.4	128.9	−117.5	119.6	−1.4	84.4	−71.4
$HCl_2SiSiH_2Cl \leftrightarrow SiH_3Cl+SiCl_2$	SiSiClH H H ClCl	C_1	2.314	2.072	1.465	1.467	1.645	2.056	2.056	128.3	96.6	105.1	48.9	119.1	120.8	−120.2	118.8	19.4	90.2	−50.9
$Cl_3SiSiH_3 \leftrightarrow SiHCl_3+SiH_2$	SiSiClClClH H H	C_s	2.823	2.034	2.019	2.019	1.811	1.503	1.503	134.1	95.7	95.7	28.4	96.8	96.8	−123.1	123.1	0.0	48.3	−48.3
$Cl_3SiSiH_3 \leftrightarrow SiH_3Cl+SiCl_2$	SiSiH H H ClClCl	C_s	2.545	1.476	1.470	1.470	2.334	2.062	2.062	144.5	92.3	92.3	56.6	125.8	125.8	−121.8	121.8	0.0	80.4	−80.4
$HCl_2SiSiHCl_2 \leftrightarrow SiHCl_3+SiHCl$	SiSiClH ClClClH	C_1	2.574	2.079	1.461	2.051	2.419	2.062	1.484	156.2	88.4	93.1	51.5	122.0	126.5	−112.7	126.9	−8.5	72.8	−70.6
$HCl_2SiSiHCl_2 \leftrightarrow SiH_2Cl_2+SiCl_2$	SiSiClClH H ClCl	C_1	2.336	2.062	2.052	1.462	1.694	2.053	2.056	130.2	104.7	96.8	45.6	119.5	115.9	−120.1	122.4	−22.6	43.5	−90.7
$Cl_3SiSiH_2Cl \leftrightarrow SiCl_4+SiH_2$	SiSiClClClClH H	C_s	2.822	2.060	2.034	2.034	2.473	1.491	1.491	155.9	89.6	89.6	46.5	120.1	120.1	−121.2	121.2	0.0	62.3	−62.3
$Cl_3SiSiH_2Cl \leftrightarrow SiHCl_3+SiHCl$	SiSiClClClH ClH	C_1	2.432	2.056	2.035	2.033	1.738	2.074	1.487	134.3	99.9	98.4	40.7	112.7	107.1	−120.2	122.2	−11.8	57.3	−57.1
$Cl_3SiSiH_2Cl \leftrightarrow SiH_2Cl_2+SiCl_2$	SiSiClH H ClClCl	C_s	2.460	2.088	1.466	1.466	2.290	2.052	2.052	149.1	93.7	93.7	58.4	125.8	125.8	−118.9	118.9	0.0	83.7	−83.7
$Cl_3SiSiHCl_2 \leftrightarrow SiCl_4+SiHCl$	SiSiClClClClClH	C_1	2.717	2.064	2.040	2.045	2.533	2.061	1.489	158.5	89.4	89.4	47.7	122.8	122.6	−121.2	120.6	−0.3	76.5	−58.0
$Cl_3SiSiHCl_2 \leftrightarrow SiHCl_3+SiCl_2$[b]	SiSiClClClH ClCl	C_1	2.335	2.057	2.047	2.030	1.710	2.053	2.050	129.7	103.0	101.1	45.3	115.5	118.9	−117.5	124.7	−24.1	44.9	−88.3
$Cl_3SiSiHCl_2 \leftrightarrow SiHCl_3+SiCl_2$[c]	SiSiH ClClClClCl	C_s	2.575	1.462	2.058	2.058	2.546	2.046	2.046	157.2	91.2	91.2	50.4	124.2	124.2	−120.8	120.8	0.0	75.9	−75.9
$Cl_3SiSiCl_3 \leftrightarrow SiCl_4+SiCl_2$	SiSiClClClClClCl	C_s	2.544	2.071	2.053	2.053	2.495	2.044	2.044	157.3	91.3	91.3	51.3	124.4	124.4	−120.9	120.9	0.0	77.2	−77.2
Transition States with Structure of Figure 2b																				
$H_3SiSiH_3 \leftrightarrow H_3SiSiH+H_2$	SiSiH H H H H H	C_1	2.332	1.476	1.475	1.477	1.481	1.634	1.537	109.6	115.4	106.7	111.5	77.7	103.7	−121.5	117.0	103.3	−176.8	−148.1
$H_2ClSiSiH_3 \leftrightarrow H_3SiSiCl+H_2$	SiSiH H H ClH H	C_1	2.412	1.474	1.475	1.476	2.109	1.650	1.572	102.4	119.8	106.6	102.0	53.8	91.5	−118.5	115.4	77.8	165.4	178.2
$H_2ClSiSiH_3 \leftrightarrow H_2ClSiSiH+H_2$	SiSiClH H H H H	C_1	2.323	2.071	1.472	1.474	1.482	1.637	1.544	110.1	115.5	108.2	109.4	73.9	100.6	−119.5	116.7	110.7	−170.4	−143.2
$H_2ClSiSiH_2Cl \leftrightarrow H_2ClSiSiCl+H_2$	SiSiH ClH ClH H	C_1	2.386	1.470	2.066	1.474	2.095	1.648	1.572	104.2	121.7	105.3	104.8	54.7	91.5	−118.5	116.7	75.6	162.9	177.3
$HCl_2SiSiH_3 \leftrightarrow HCl_2SiSiH+H_2$	SiSiClH ClH H H	C_1	2.316	2.058	1.468	2.056	1.481	1.623	1.532	109.2	118.9	106.8	109.3	74.6	101.7	−120.4	118.3	95.5	175.0	−155.6
$HCl_2SiSiH_2Cl \leftrightarrow HCl_2SiSiCl+H_2$	SiSiClH ClClH H	C_1	2.368	2.054	1.468	2.051	2.092	1.648	1.555	105.6	121.5	105.6	104.6	55.4	93.2	−118.4	116.5	82.2	168.9	−173.6
$Cl_3SiSiH_3 \leftrightarrow Cl_3SiSiH+H_2$	SiSiClClClH H H	C_1	2.309	2.051	2.048	2.049	1.478	1.623	1.527	110.3	115.9	107.8	109.9	75.0	101.7	−120.6	117.4	101.5	−178.8	−148.0
$Cl_3SiSiH_2Cl \leftrightarrow Cl_3SiSiCl+H_2$	SiSiClClClClH H	C_1	2.369	2.047	2.046	2.045	2.084	1.651	1.551	105.6	120.5	106.0	105.0	53.2	92.1	−118.6	115.3	82.4	168.8	−173.4
Transition States with Structure of Figure 2c																				
$SiH_4+SiHCl \leftrightarrow SiH_3Cl+SiH_2$	SiSiH H H ClH H	C_1	2.933	1.472	1.480	1.464	2.309	1.585	1.503	132.5	104.7	93.5	51.9	29.0	82.8	−122.8	123.5	−21.9	136.9	−119.2
$SiH_3Cl+SiHCl \leftrightarrow SiH_2Cl_2+SiH_2$	SiSiH ClH ClH H	C_1	2.918	1.466	2.080	1.463	2.337	1.583	1.503	137.1	105.2	92.8	49.7	29.2	83.2	−119.2	126.2	−21.3	140.7	−117.4
$SiH_3Cl+SiHCl \leftrightarrow SiH_4+SiCl_2$	SiSiH H H ClH Cl	C_1	2.963	1.470	1.470	1.477	2.312	1.602	2.102	127.4	103.0	98.0	52.4	27.1	89.1	−129.2	114.0	34.4	−167.3	−67.0
$SiH_2Cl_2+SiHCl \leftrightarrow SiHCl_3+SiH_2$	SiSiH ClClClH H	C_1	2.868	1.460	2.046	2.066	2.310	1.600	1.500	133.8	104.4	99.9	51.7	28.9	81.8	−128.4	112.4	26.8	−173.9	−69.9
$SiH_2Cl_2+SiHCl \leftrightarrow SiH_3Cl+SiCl_2$	SiSiH ClH ClH Cl	C_1	2.967	1.465	2.078	1.464	2.349	1.613	2.084	135.5	105.0	92.7	49.8	26.7	93.4	−118.7	125.8	−21.8	145.0	−119.6
$SiHCl_3+SiHCl \leftrightarrow SiCl_4+SiH_2$	SiSiClClClClH H	C_1	2.825	2.064	2.040	2.069	2.314	1.582	1.500	133.1	108.1	97.2	51.5	31.2	76.3	−136.6	108.0	43.8	−170.6	−56.3
$SiHCl_3+SiHCl \leftrightarrow SiH_2Cl_2+SiCl_2$	SiSiH ClClClH Cl	C1	2.962	1.457	2.049	2.054	2.305	1.663	2.075	132.3	99.9	103.9	52.4	24.8	97.8	−119.2	119.2	7.6	−172.2	−87.6
$SiCl_4+SiHCl \leftrightarrow SiHCl_3+SiCl_2$	SiSiClClClClH Cl	C_1	2.962	2.052	2.035	2.061	2.293	1.659	2.077	132.2	100.7	103.7	52.8	24.2	95.5	−126.1	116.4	−28.3	−157.2	−68.6
Transition States with Structure of Figure 2d																				
$H_3SiSiH_3 \leftrightarrow SiH_4+SiH_2$	SiSiH H H H H H	C_1	2.690	1.464	1.469	1.472	1.510	1.608	1.505	98.3	109.6	117.5	65.2	33.8	72.3	−115.9	116.7	58.2	−167.8	−47.1
$H_2ClSiSiH_3 \leftrightarrow SiH_3Cl+SiH_2$	SiSiClH H H H H	C_1	2.813	2.038	1.462	1.469	1.511	1.672	1.503	102.7	98.0	125.7	61.3	28.5	81.8	−114.8	121.5	66.0	−134.4	−34.0

[a] Bond lengths in angstroms; bond angles and dihedral angles in degrees. Atom numbering as shown in Figure 2 i.e. SiH ClH H H Cl means the atoms labeled 1 and 2 are Si, atoms 3, 5, 6, and 7 are H, and atoms 4 and 8 are Cl in any of the structures of Figure 2. [b] Transition state corresponding to insertion into Si−H bond. [c] Transition state corresponding to insertion into Si−Cl bond.

TABLE 4: Unscaled MP2/6-31G(d,p) Vibrational Frequencies[a]

Stable Molecules																		
H_3SiSiH	95	402	409	455	755	925	974	998	2163	2293	2306	2328						
$H_3SiSiCl$	70	144	397	416	509	547	918	972	986	2303	2322	2324						
$H_2ClSiSiH$	136	183	322	391	565	667	739	867	958	2148	2304	2320						
$H_2ClSiSiCl$	44	88	168	356	438	528	563	716	846	968	2315	2335						
HCl_2SiSiH	42	144	190	292	411	526	595	683	763	848	2165	2348						
$HCl_2SiSiCl$	22	82	112	142	217	443	535	549	588	773	819	2348						
Cl_3SiSiH	30	109	184	184	209	233	365	563	593	600	712	2185						
$Cl_3SiSiCl$	11	75	85	141	180	188	236	366	544	573	599	614						
H_3SiSiH_3	144	384	384	460	667	667	901	980	985	985	1002	1002	2318	2328	2333	2333	2341	2341
$H_2ClSiSiH_3$	115	128	372	436	542	571	627	742	861	943	987	988	1005	2325	2339	2345	2347	2355
HCl_2SiSiH_3	109	121	152	201	414	534	550	567	607	809	841	939	984	987	2333	2353	2356	2361
$H_2ClSiSiH_2Cl$	47	81	165	367	468	560	573	598	712	745	810	913	991	998	2345	2349	2359	2367
HCl_2SiSiH_2Cl	39	71	146	156	211	428	517	552	584	607	717	780	838	893	985	2349	2365	2370
Cl_3SiSiH_3	109	109	124	188	188	211	383	539	539	592	625	625	927	983	983	2340	2363	2363
$HCl_2SiSiHCl_2$	23	64	125	130	165	194	241	455	532	591	602	617	728	826	829	863	2371	2372
Cl_3SiSiH_2Cl	39	66	110	142	186	195	234	386	509	554	604	624	626	727	871	982	2353	2373
$Cl_3SiSiHCl_2$	27	66	77	132	141	183	210	211	262	388	521	610	613	628	636	806	830	2372
$Cl_3SiSiCl_3$	28	68	68	130	130	136	184	184	225	225	254	368	484	625	625	637	637	656
Transition States with Structure of Figure 2a																		
$H_3SiSiH_3 \leftrightarrow SiH_4 + SiH_2$	192i	197	361	519	617	692	827	911	974	1018	1051	1456	1652	2247	2268	2296	2353	2382
$H_2ClSiSiH_3 \leftrightarrow SiH_3Cl + SiH_2$[b]	64i	109	163	403	520	593	620	704	787	942	997	1026	1299	2045	2179	2199	2366	2418
$H_2ClSiSiH_3 \leftrightarrow SiH_3Cl + SiH_2$[c]	271i	195	250	278	395	608	644	664	763	898	1017	1057	1101	2253	2274	2281	2341	2378
$H_2ClSiSiH_3 \leftrightarrow SiH_4 + SiHCl$	470i	112	178	405	550	569	652	765	832	934	967	1059	1319	1673	2291	2313	2333	2375
$H_2ClSiSiH_2Cl \leftrightarrow SiH_2Cl_2 + SiH_2$	120i	76	154	237	432	487	573	605	712	814	900	970	1075	1290	1958	2029	2349	2356
$H_2ClSiSiH_2Cl \leftrightarrow SiH_3Cl + SiHCl$	332i	71	114	269	396	479	534	596	732	817	837	900	939	1243	1702	2317	2357	2393
$HCl_2SiSiH_3 \leftrightarrow SiH_2Cl_2 + SiH_2$	122i	77	164	165	209	506	536	593	648	731	742	905	1024	1268	2086	2185	2198	2392
$HCl_2SiSiH_3 \leftrightarrow SiH_3Cl + SiHCl$	284i	70	135	215	271	384	552	622	642	739	831	900	1044	1100	2268	2294	2333	2369
$HCl_2SiSiH_3 \leftrightarrow SiH_4 + SiCl_2$	488i	105	155	168	310	443	539	579	612	788	939	961	1060	1264	1658	2314	2320	2388
$HCl_2SiSiH_2Cl \leftrightarrow SiHCl_3 + SiH_2$	185i	89	133	179	222	270	304	441	516	577	580	690	730	909	1037	2253	2276	2418
$HCl_2SiSiH_2Cl \leftrightarrow SiH_2Cl_2 + SiHCl$[b]	254i	55	69	163	200	281	477	530	567	612	700	757	826	918	1361	1628	2301	2379
$HCl_2SiSiH_2Cl \leftrightarrow SiH_2Cl_2 + SiHCl$[c]	187i	54	122	159	204	279	400	478	501	575	676	817	829	932	962	2301	2344	2393
$HCl_2SiSiH_2Cl \leftrightarrow SiH_3Cl + SiCl_2$	373i	54	107	123	185	346	462	522	606	627	694	815	897	922	1069	1719	2350	2399
$Cl_3SiSiH_3 \leftrightarrow SiHCl_3 + SiH_2$	106i	76	106	156	187	195	242	479	520	616	627	660	767	1026	1217	2115	2188	2201
$Cl_3SiSiH_3 \leftrightarrow SiH_3Cl + SiCl_2$	290i	61	125	151	179	186	285	378	561	569	642	715	895	1036	1093	2312	2332	2368
$HCl_2SiSiHCl_2 \leftrightarrow SiHCl_3 + SiHCl$	155i	47	82	119	164	196	256	264	426	506	556	570	640	708	816	960	2283	2388
$HCl_2SiSiHCl_2 \leftrightarrow SiH_2Cl_2 + SiCl_2$	256i	46	69	110	150	213	250	332	518	562	598	615	652	821	871	1246	1643	2401
$Cl_3SiSiH_2Cl \leftrightarrow SiCl_4 + SiH_2$	218i	86	112	120	194	223	224	267	288	390	535	558	578	654	682	1032	2239	2261
$Cl_3SiSiH_2Cl \leftrightarrow SiHCl_3 + SiHCl$	153i	54	64	135	169	198	222	260	445	542	570	584	649	737	827	1460	1630	2266
$Cl_3SiSiH_2Cl \leftrightarrow SiH_2Cl_2 + SiCl_2$	224i	45	105	138	147	167	224	287	391	462	511	597	605	830	920	949	2342	2389
$Cl_3SiSiHCl_2 \leftrightarrow SiCl_4 + SiHCl$	195i	46	64	102	125	172	203	229	232	259	385	524	550	569	614	643	829	2254
$Cl_3SiSiHCl_2 \leftrightarrow SiHCl_3 + SiCl_2$[b]	263i	26	68	98	135	164	185	218	232	326	484	564	602	617	635	743	1214	1634
$Cl_3SiSiHCl_2 \leftrightarrow SiHCl_3 + SiCl_2$[c]	179i	52	58	90	120	131	166	177	240	293	393	537	576	596	620	921	928	2373
$Cl_3SiSiCl_3 \leftrightarrow SiCl_4 + SiCl_2$	153i	48	55	84	118	134	159	180	229	230	248	274	375	509	557	593	602	631
Transition States with Structure of Figure 2b																		
$H_3SiSiH_3 \leftrightarrow H_3SiSiH + H_2$	1021i	170	358	430	463	617	728	874	945	978	1017	1078	1812	2167	2298	2322	2334	2338
$H_2ClSiSiH_3 \leftrightarrow H_3SiSiCl + H_2$	1041i	102	150	321	474	519	570	630	708	940	966	1012	1156	1769	2020	2323	2337	2345
$H_2ClSiSiH_3 \leftrightarrow H_2ClSiSiH + H_2$	982i	120	169	357	394	470	562	671	799	875	892	969	1072	1818	2151	2297	2334	2353
$H_2ClSiSiH_2Cl \leftrightarrow H_2ClSiSiCl + H_2$	1048i	61	89	200	324	448	523	551	583	704	769	882	967	1156	1780	2025	2336	2358
$HCl_2SiSiH_3 \leftrightarrow HCl_2SiSiH + H_2$	1067i	116	137	176	220	348	451	558	581	629	819	853	872	1055	1817	2174	2303	2363
$HCl_2SiSiH_2Cl \leftrightarrow HCl_2SiSiCl + H_2$	1061i	48	76	151	176	223	302	502	525	576	607	699	779	870	1106	1750	2062	2364
$Cl_3SiSiH_3 \leftrightarrow Cl_3SiSiH + H_2$	1088i	107	129	169	195	203	221	362	397	581	582	603	660	857	1045	1822	2188	2319
$Cl_3SiSiH_2Cl \leftrightarrow Cl_3SiSiCl + H_2$	1035i	41	65	142	150	199	204	227	311	471	534	590	601	632	735	1103	1743	2064
Transition States with Structure of Figure 2c																		
$SiH_4 + SiHCl \leftrightarrow SiH_3Cl + SiH_2$	389i	178	248	357	361	684	703	752	916	975	1022	1125	1167	1937	2187	2293	2329	2401
$SiH_3Cl + SiHCl \leftrightarrow SiH_2Cl_2 + SiH_2$	161i	139	200	272	348	426	533	636	746	788	963	1023	1038	1197	1919	2191	2354	2399
$SiH_3Cl + SiHCl \leftrightarrow SiH_4 + SiCl_2$	380i	61	156	183	323	351	494	532	678	908	961	993	1122	1185	1857	2310	2341	2384
$SiH_2Cl_2 + SiHCl \leftrightarrow SiHCl_3 + SiH_2$	113i	87	113	171	216	343	373	507	550	612	766	833	978	993	1285	1868	2205	2378
$SiH_2Cl_2 + SiHCl \leftrightarrow SiH_3Cl + SiCl_2$	168i	85	107	166	196	328	353	514	531	561	776	887	1008	1018	1250	1801	2360	2392
$SiHCl_3 + SiHCl \leftrightarrow SiCl_4 + SiH_2$	85i	115	141	166	199	220	238	305	369	495	532	594	629	778	1027	1231	1906	2199
$SiHCl_3 + SiHCl \leftrightarrow SiH_2Cl_2 + SiCl_2$	171i	35	53	124	157	174	230	350	380	500	537	622	859	910	943	1330	1732	2392
$SiCl_4 + SiHCl \leftrightarrow SiHCl_3 + SiCl_2$	156i	32	55	128	152	167	207	227	232	316	371	490	534	582	636	865	1345	1772
Transition States with Structure of Figure 2d																		
$H_3SiSiH_3 \leftrightarrow SiH_4 + SiH_2$	144i	105	359	560	665	694	949	965	1001	1011	1077	1325	1854	2160	2177	2351	2375	2396
$H_2ClSiSiH_3 \leftrightarrow SiH_3Cl + SiH_2$	137i	143	222	271	568	582	661	746	862	944	999	1035	1443	1862	2154	2193	2368	2410

[a] Frequencies are in units of cm^{-1} and are unscaled. Degenerate frequencies are simply repeated an appropriate number of times. [b] Transition state corresponding to insertion into Si−H bond. [c] Transition state corresponding to insertion into Si−Cl bond.

was derived from the experimentally established heat of reaction for Si_2H_6 decomposition and referenced to the value of 19.1 kcal/mol for Si_2H_6.[4] So, if we changed the value of $\Delta H_f°$ for Si_2H_6, we would need to make a corresponding change in $\Delta H_f°$ for SiH_2. The result of this is that the heat of reaction for all of the reactions considered here is unaffected by the value of $\Delta H_f°$ for Si_2H_6, provided that the value used for SiH_2 is consistent with it.

The heats of formation in Table 5 can be reasonably reproduced by a bond additivity scheme. We can write the heats

TABLE 5: Heats of Formation Calculated Using Isodesmic Reactions[a]

molecule	MP2 6-31G(d,p)	MP2 6-31+G(2df,p)	MP4 6-31+G(2df,p)	G2(MP2)	G2	S(298)
H_3SiSiH	76.0	75.1	75.1	75.4	75.4	67.7
$H_3SiSiCl$	27.2	25.8	26.0	26.3	26.8	76.0
$H_2ClSiSiH$	34.4	33.6	33.8	33.9	34.1	74.5
$H_2ClSiSiCl$	−14.3	−15.7	−15.3	−15.2	−14.6	83.4
HCl_2SiSiH	−8.8	−10.4	−9.8	−10.1	−9.6	83.0
$HCl_2SiSiCl$	−57.3	−58.9	−58.3	−58.5		92.1
Cl_3SiSiH	−53.1	−53.8	−53.3	−53.5		91.1
$Cl_3SiSiCl$	−101.3	−102.8				100.2
$H_2ClSiSiH_3$	−21.3	−21.3	−21.1	−21.1	−21.0	76.3
$H_2ClSiSiH_2Cl$	−61.7	−61.6	−61.3	−61.4	−61.3	83.0
HCl_2SiSiH_3	−64.2	−64.2	−63.9	−64.0	−63.8	83.7
HCl_2SiSiH_2Cl	−104.1	−104.2	−103.8	−104.1		91.8
Cl_3SiSiH_3	−108.2	−108.0	−107.6	−107.9		88.5
$HCl_2SiSiHCl_2$	−146.4	−146.8				98.0
Cl_3SiSiH_2Cl	−147.9	−147.8				98.4
$Cl_3SiSiHCl_2$	−190.1	−190.3				105.5
$Cl_3SiSiCl_3$	−233.8	−233.9				108.3

[a] Heats of formation in kcal/mol at 298.15 K and 1 atm calculated using isodesmic reactions given in text and total energies, thermal, and zero-point energies from Table 1. Entropies are in cal/(mol/K) calculated using the unscaled MP2/6-31G(d,p) vibrational frequencies. Reference values for calculating heats of formation were $\Delta H_f(SiH_4) = 8.2$ kcal/mol,[30] $\Delta H_f(SiCl_4) = -158.4$ kcal/mol,[30] $\Delta H_f(SiH_2) = 65.2$ kcal/mol,[4] and $\Delta H_f(Si_2H_6) = 19.1$ kcal/mol.[31] Entries left blank were not calculated due to computational expense.

of formation for the Si−H−Cl compounds as

$$\Delta H_f^\circ = \Delta H_{Si-Si} n_{Si-Si} + \Delta H_{Si-H} n_{Si-H} + \Delta H_{Si-Cl} n_{Si-Cl} + \Delta H_{Si(d)-Si} n_{Si(d)-Si} + \Delta H_{Si(d)-H} n_{Si(d)-H} + \Delta H_{Si(d)-Cl} n_{Si(d)-Cl}$$

where n_{Si-Si} is the number of Si−Si bonds, n_{Si-H} is the number of Si−H bonds, n_{Si-Cl} is the number of Si−Cl bonds, $n_{Si(d)-Si}$ is the number of Si−Si bonds where one of the silicon atoms is divalent, $n_{Si(d)-H}$ is the number of Si−H bonds where the silicon atom is divalent, and $n_{Si(d)-Cl}$ is the number of Si−Cl bonds where the silicon atom is divalent. The ΔH values are the corresponding increments to the heat of formation. Values of $\Delta H_{Si-Si} = 6.23$ kcal/mol, $\Delta H_{Si-H} = 2.50$ kcal/mol, $\Delta H_{Si-Cl} = -39.84$, $\Delta H_{Si(d)-S} = 29.95$ kcal/mol, $\Delta H_{Si(d)-H} = 29.67$ kcal/mol, and $\Delta H_{Si(d)-Cl} = 21.66$ kcal/mol were obtained by a least-squares fit of the above expression to the heats of formation of the compounds in Table 5, plus disilane, the chlorinated silanes SiH_nCl_{4-n}, and the chlorinated silylenes SiH_nCl_{2-n}. These parameters fit the heats of formation of the 26 compounds considered to within an average absolute error of 1.1 kcal/mol and a maximum absolute error of 2.3 kcal/mol. This forms a reasonable basis for a bond additivity scheme that could be used to predict heats of formation for larger Si−H−Cl compounds.

Decomposition Reaction Energetics and Kinetics. The heats of reaction, forward and reverse reaction barriers, and estimated rate parameters at 1000 K for all of the thermal decomposition reactions considered are presented in Table 6. The reverse barriers are obtained by subtracting the calculated energy, including zero-point energy, of the products from that of the transition state. A negative barrier means that the transition structure is lower in energy than the separated products. It is still, of course, higher in energy than the minimum energy cluster between the products. The forward barrier is obtained by adding the reverse barrier to the overall energy change for reaction. This was obtained from the energies of formation of reactants and products at 0 K using the isodesmic reactions presented above. The insertion barriers were more sensitive to the level of calculation than the heats of formation, but are still reasonably consistent from the MP2/6-31+G(2df,p) to the G2 levels. The barriers increase by an average of 0.3 kcal/mol from the G2(MP2) to the G2 level, decreasing in only one case. Likewise, the barriers increase by an average of 0.5 kcal/mol from the MP4/6-31+G(2df,p) level to the G2 level, decreasing in only three cases. The barriers increase in all cases from the MP2/6-31+G(2df,p) level to the G2 level, by an average of 1.8 kcal/mol, with the increases ranging from 0.3 to 3.5 kcal/mol. For estimating rate parameters, the barriers at the G2 level were used for compounds with two or fewer chlorines, and the barriers at the G2(MP2) level were used for the compounds with three chlorines. For those with four or more chlorines, the average increase of 1.8 kcal/mol was added to the barriers at the MP2/6-31+G(2df,p) level. These are the barriers given in the column labeled “best value” in Table 6.

The estimated rate constants, activation energies, and pre-exponential factors were obtained from conventional transition state theory calculations[32] treating all vibrations as harmonic oscillators and all rotations as rigid rotors. Improved treatment of internal rotations and low vibrational frequencies, as well as a variational treatment for those reactions with negative calculated barriers, would be required to make more accurate estimates of rate constants, but would go beyond the scope of this paper. Note that ratios of rates of competing reactions, i.e., different decomposition reactions of a single reactant, depend only on the energies and partition functions of the transition states for the competing paths and not those of the reacting molecules. Many of these reactions are likely to be in the pressure dependent falloff regime at conditions of practical interest, so unimolecular rate theory calculations of the pressure and temperature dependence of the reactions are needed to fully characterize them. This also falls outside the scope of this work. Figure 3 gives a diagram of the energetics for the $Si_2H_3Cl_3$ system to illustrate typical results for the various possible reaction paths. Note that for this system, as well as most of the others, the energetic barriers for different reaction paths lie quite close together. The observations below are based on the energetics as presented in Table 5, realizing that relative changes of a few kcal/mol in the energetics would change the results significantly. However, these observations still represent the best information that is available at this time for the reactions considered.

H_3SiSiH_3 Decomposition. The results for disilane decomposition agree well with the previous studies cited above. Silylene elimination from disilane is predicted to occur via a loose transition state. The saddle points located for both SiH_2 elimination geometries lie well below the separated products. The rate parameters in Table 5 are those obtained with the

TABLE 6: Thermal Decomposition Barriers and Rate Parameters[a]

			reverse barrier									
reaction	TS type	ΔH_{rxn}	MP2 6-31G(d,p)	MP2 6-31+G(2df,p)	MP4 6-31+G(2df,p)	G2(MP2)	G2	best value	forward barrier	*k*(1000 K)	log A	E_a
$H_3SiSiH_3 \rightarrow SiH_4 + SiH_2$	a	54.3	−3.8	−8.8	−7.5	−6.7	−6.4	−6.44	46.7	7537	14.2	47.1
$H_3SiSiH_3 \rightarrow SiH_4 + SiH_2$	d	54.3	−5.0	−9.6	−8.5	−8.7	−8.2	−8.2	44.9	28740	14.4	45.3
$H_3SiSiH_3 \rightarrow H_3SiSiH + H_2$	b	56.3	1.1	−2.7	−1.0	−1.0	−0.5	−0.5	53.8	430	14.7	55.0
$H_2ClSiSiH_3 \rightarrow SiH_3Cl + SiH_2$[b]	a	54.2	−2.2	−6.8	−6.0	−6.1	−5.8	−5.8	47.5	3351	14.0	48.0
$H_2ClSiSiH_3 \rightarrow SiH_3Cl + SiH_2$[c]	a	54.2	4.9	−3.0	−1.3	−0.3	0.0	0.0	53.3	32	13.3	53.9
$H_2ClSiSiH_3 \rightarrow SiH_3Cl + SiH_2$[b]	d	54.2	−3.4	−7.8	−6.9	−7.5	−7.0	−7.0	46.3	4226	13.8	46.6
$H_2ClSiSiH_3 \rightarrow SiH_4 + SiHCl$	a	44.4	8.5	3.2	4.4	4.7	4.8	4.8	48.4	505	13.4	48.8
$H_2ClSiSiH_3 \rightarrow H_3SiSiCl + H_2$	b	47.8	12.0	7.6	9.4	9.4	9.8	9.8	55.7	33	14.0	57.0
$H_2ClSiSiH_3 \rightarrow H_2ClSiSiH + H_2$	b	55.2	1.1	−3.0	−1.3	−1.1	−0.7	−0.7	52.6	396	14.4	53.9
$H_2ClSiSiH_2Cl \rightarrow SiH_2Cl_2 + SiH_2$	a	52.2	0.9	−7.5	−5.4	−4.3	−3.9	−4.0	47.4	457	13.1	47.6
$H_2ClSiSiH_2Cl \rightarrow SiH_3Cl + SiHCl$	a	44.4	4.7	−0.9	0.5	0.9	0.9	0.9	44.9	7737	13.8	45.3
$H_2ClSiSiH_2Cl \rightarrow H_2ClSiSiCl + H_2$	b	46.7	12.3	7.7	9.6	9.7	10.0	10.0	54.8	81	14.2	56.0
$HCl_2SiSiH_3 \rightarrow SiH_2Cl_2 + SiH_2$	a	54.7	−0.6	−5.6	−4.8	−5.2	−4.8	−4.8	49.3	1503	14.1	49.8
$HCl_2SiSiH_3 \rightarrow SiH_3Cl + SiHCl$	a	47.0	10.8	2.3	4.0	5.0	5.1	5.1	51.7	226	13.8	52.1
$HCl_2SiSiH_3 \rightarrow SiH_4 + SiCl_2$	a	33.6	25.2	20.3	21.1	20.6	20.5	20.5	53.5	33	13.3	53.8
$HCl_2SiSiH_3 \rightarrow HCl_2SiSiH + H_2$	b	54.2	1.1	−2.6	−1.0	−0.5	−0.3	−0.3	52.2	485	14.4	53.5
$HCl_2SiSiH_2Cl \rightarrow SiHCl_3 + SiH_2$	a	52.3	4.6	−4.2	−2.4	−1.5		−1.5	50.0	83	13.1	50.9
$HCl_2SiSiH_2Cl \rightarrow SiH_2Cl_2 + SiHCl$[b]	a	44.5	6.9	0.8	2.1	2.4		2.4	46.6	903	13.3	47.1
$HCl_2SiSiH_2Cl \rightarrow SiH_2Cl_2 + SiHCl$[c]	a	44.5	7.9	−1.2	0.9	1.9		2.0	46.2	1530	13.4	46.8
$HCl_2SiSiH_2Cl \rightarrow SiH_3Cl + SiCl_2$	a	32.8	21.0	15.8	16.9	16.3		16.3	48.8	238	13.1	49.3
$HCl_2SiSiH_2Cl \rightarrow HCl_2SiSiCl + H_2$	b	45.6	12.7	7.9	9.8	9.9		9.9	53.6	80	13.9	54.9
$Cl_3SiSiH_3 \rightarrow SiHCl_3 + SiH_2$	a	56.1	−0.4	−5.1	−4.3	−4.8		−4.8	50.7	773	14.1	51.3
$Cl_3SiSiH_3 \rightarrow SiH_3Cl + SiCl_2$	a	36.6	18.9	10.5	12.1	12.6		12.6	49.2	1656	14.1	49.6
$Cl_3SiSiH_3 \rightarrow Cl_3SiSiH + H_2$	b	54.5	2.0	−2.3	−0.5	−0.4		−0.4	52.2	421	14.3	53.5
$HCl_2SiSiHCl_2 \rightarrow SiHCl_3 + SiHCl$	a	44.3	10.4	1.0				2.8	46.9	2124	13.7	47.7
$HCl_2SiSiHCl_2 \rightarrow SiH_2Cl_2 + SiCl_2$	a	32.2	22.8	17.30				19.1	51.3	92	13.3	51.7
$Cl_3SiSiH_2Cl \rightarrow SiCl_4 + SiH_2$	a	54.6	7.7	−1.2				0.7	54.5	10	13.2	55.5
$Cl_3SiSiH_2Cl \rightarrow SiHCl_3 + SiHCl$	a	45.3	8.5	2.4				4.2	49.4	420	13.5	49.8
$Cl_3SiSiH_2Cl \rightarrow SiH_2Cl_2 + SiCl_2$	a	33.2	17.4	8.6				10.4	43.7	12587	13.8	44.3
$Cl_3SiSiH_2Cl \rightarrow Cl_3SiSiCl + H_2$	b	45.1	13.7	8.7				10.5	53.7	228	14.4	55.0
$Cl_3SiSiHCl_2 \rightarrow SiCl_4 + SiHCl$	a	46.6	12.6	3.2				5.0	51.3	180	13.7	52.3
$Cl_3SiSiHCl_2 \rightarrow SiHCl_3 + SiCl_2$[b]	a	33.1	24.6	18.8				20.6	53.9	27	13.3	54.3
$Cl_3SiSiHCl_2 \rightarrow SiHCl_3 + SiCl_2$[c]	a	33.1	18.5	10.2				12.1	45.3	7756	13.9	45.9
$Cl_3SiSiCl_3 \rightarrow SiCl_4 + SiCl_2$	a	35.4	20.1	10.7				12.5	48.1	3095	14.2	48.8

[a] Energies are in kcal/mol. ΔH_{rxn} is the standard heat of reaction at 298 K calculated from the heats of formation in Table 4. Forward and reverse reaction barriers at 0 K, including zero-point energy, calculated as described in the text. Transition-state type refers to the structures of Figure 2. Estimated rate parameters are at 1000 K. *k* and *A* are in s^{-1}, E_a is in kcal/mol. Entries left blank were not calculated due to computational expense. [b] Transition state corresponding to insertion into a Si−H bond. [c] Transition state corresponding to insertion into a Si−Cl bond.

transition states located at the saddle points. A variational treatment with the transition state located closer to the separated products would be needed to make reasonable rate constant predictions for this reaction over wide temperature ranges.[4] However, at high enough temperatures, the transition state will tighten until it lies at or near the saddle points located on the potential surface. At sufficiently high temperatures, greater than around 1000 K in this case, tight transition state calculations will then provide reasonable estimates of the rate parameters. The transition state for H_2 elimination is predicted to lie 0.5 kcal/mol below the separated products, giving an activation energy of about 55 kcal/mol, consistent with shock tube measurements of this reaction.[33] This reaction is slower than the silylene elimination, but is known to play a role in the mechanism of thermal decomposition of silane.[34]

$H_2ClSiSiH_3$ Decomposition. Chlorodisilane is predicted to decompose by SiH_2 and SiHCl elimination, with SiH_2 elimination being faster. As was the case for disilane, the saddle point on the path for SiH_2 elimination via an H atom shift lies below the separated products. At low temperatures, this reaction should occur via a loose transition state with an activation energy near the heat of reaction. At higher temperatures, the transition state will tighten until the activation energy is near 48 kcal/mol and the preexponential drops to near 10^{14} s^{-1}, as predicted by the tight transition state calculations. By contrast, the barrier for SiH_2 elimination via a Cl atom shift is essentially isoenergetic with the products. That reaction would therefore proceed through a tight transition state and would be much slower than the path involving transfer of an H atom. SiHCl elimination is predicted to have an activation energy comparable to the high-temperature activation energy for silylene elimination. Jenkins et al.[22] found that the ratio of SiH_2 elimination to SiHCl elimination was 0.8 at 663 K, based on an analysis of the final products of $H_2ClSiSiH_3$ decomposition and reasonable mechanistic assumptions. This is inconsistent with our results, which predict SiH_2 elimination to be faster by a factor of at least 5, depending how the loose transition state for SiH_2 elimination is treated. An increase of 2−3 kcal/mol in the activation energy for SiH_2 elimination relative to SiHCl elimination would be required to bring our results into agreement with the branching ratio observed by Jenkins et al. It should be noted that their experiments were carried out at reduced pressure and were probably in the unimolecular falloff regime, which may have affected the observed branching ratio. Their pyrolysis experiments also took place in the presence of hot walls, which may have catalyzed reactions that would change the branching ratio or observed final products. Hydrogen elimination is predicted to be slightly slower than SiHCl elimination, with production of $H_2ClSiSiH$ strongly favored over production of $H_3SiSiCl$.

$H_2ClSiSiH_2Cl$ Decomposition. For 1,2-dichlorodisilane, SiHCl elimination is predicted to have an activation energy of 45 kcal/mol and be faster than SiH_2 elimination. Silylene elimination again will be governed by a loose transition state and should show a decreasing activation energy with increasing temperature. H_2 elimination is predicted to have an activation

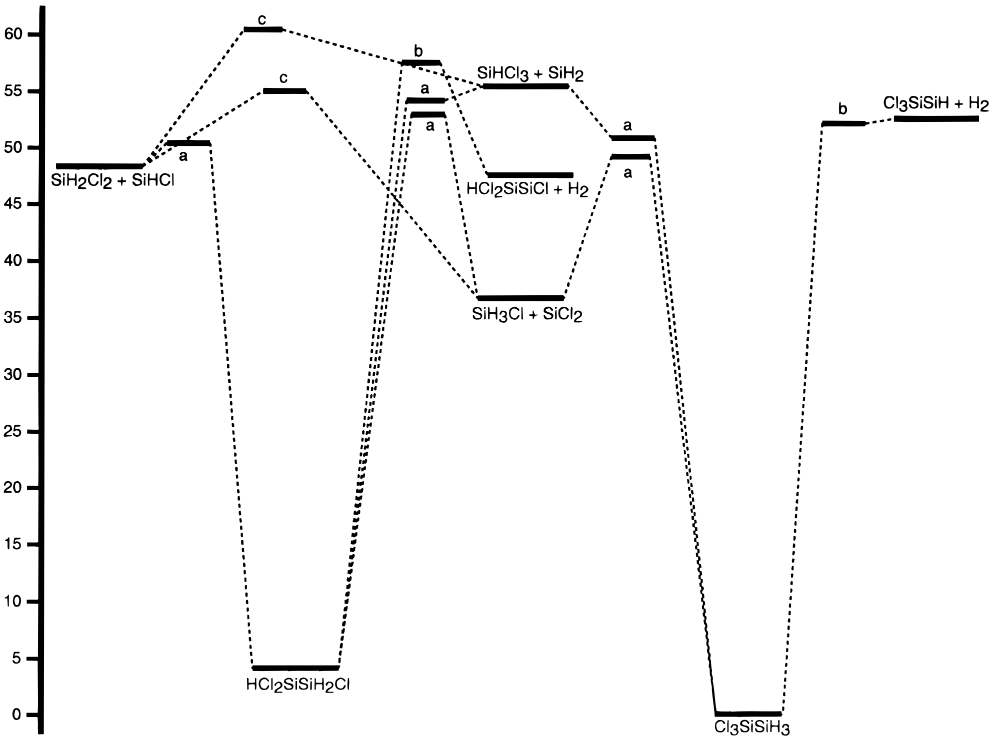

Figure 3. Diagram of energies of SiH_3Cl_3 species and saddle points on the paths connecting them. Energies are in kcal/mol at 0 K relative to Cl_3SiSiH_3. Energies of reaction and barrier heights were calculated as described in the text from the G2(MP2) energies. Transition-state labels (a, b, c) correspond to the transition-state types illustrated in Figure 2.

energy of 56 kcal/mol, making it much slower than the other reactions.

HCl_2SiSiH_3 Decomposition. Silylene elimination is predicted to be the fastest reaction, again proceeding through a loose transition state with an activation energy decreasing from nearly the heat of reaction down to 50 kcal/mol as the temperature is increased. SiHCl and H_2 elimination proceed at comparable rates with activation energies of 52 and 53 kcal/mol, respectively. $SiCl_2$ elimination is predicted to be the slowest reaction, with an activation energy near 54 kcal/mol and a relatively low preexponential factor. These predictions disagree with the observation of Jenkins et al.[22] that SiH_2 and $SiCl_2$ elimination proceeded at the same rate while SiHCl and H_2 elimination were not observed. Again, the experimental results were obtained in the presence of hot walls and at reduced pressure, and the branching ratio is based on final product analysis with assumptions about the mechanism of product production. Reconciling our results with the observation of Jenkins et al. would require at least a 4 kcal/mol reduction in the activation barrier for $SiCl_2$ elimination relative to that for SiH_2 elimination.

HCl_2SiSiH_2Cl Decomposition. The energetics of these reactions are illustrated in Figure 3. SiHCl elimination is predicted to be the fastest decomposition route, with 1,2 H atom transfer and 1,2 Cl atom transfer contributing nearly equally. The predicted activation energy is 47 kcal/mol. $SiCl_2$ elimination is the next fastest process, with an activation energy of 49 kcal/mol. Silylene elimination in this molecule can only occur via a 1,2 Cl atom transfer and is substantially slower. H_2 elimination is also slower, with a rate comparable to the silylene elimination rate at 1000 K.

Cl_3SiSiH_3 Decomposition. The energetics of this reaction are also illustrated in Figure 3. $SiCl_2$ elimination, passing through a tight transition state with an activation energy of 50 kcal/mol, is predicted to be faster than silylene elimination, which goes through a loose transition state but has a higher activation energy. H_2 elimination is slower yet, with an activation barrier 3 kcal/mol higher than $SiCl_2$ elimination.

$HCl_2SiSiHCl_2$ Decomposition. The only possible reactions are SiHCl elimination and $SiCl_2$ elimination. The SiHCl elimination is predicted to be faster, with an activation energy of 48 kcal/mol, compared to 52 kcal/mol for $SiCl_2$.

Cl_3SiSiH_2Cl Decomposition. $SiCl_2$ elimination is fastest, followed by SiHCl elimination, H_2 elimination, and SiH_2 elimination. $SiCl_2$ elimination is predicted to have an activation energy of only 44 kcal/mol.

$Cl_3SiSiHCl_2$ Decomposition. $SiCl_2$ elimination is much faster than SiHCl elimination. These reactions have activation energies of 46 and 52 kcal/mol, respectively. The $SiCl_2$ elimination occurs almost entirely by Cl atom transfer. Elimination via H atom transfer is predicted to have a barrier that is 8 kcal/mol higher than Cl atom transfer. Thus, Cl atom transfer is preferred to H atom transfer for $SiCl_2$ elimination, in contrast to SiH_2 elimination, where H atom transfer was preferred.

$Cl_3SiSiCl_3$ Decomposition. The only possible reaction is $SiCl_2$ elimination, which is predicted to occur with an activation energy of 49 kcal/mol. This is in good agreement with the value of 49.2 kcal/mol measured by Doncaster and Walsh near 600 K.[23]

Insertion and Exchange Reaction Energetics and Kinetics. Table 7 presents energetic and kinetic results for the insertion reactions which are the reverse of the thermal decomposition reactions and direct exchange reactions between chlorinated silylenes and chlorinated silanes. The barriers and rate constants are determined by the same methods as for the thermal decomposition reactions. Direct exchange reactions in which a hydrogen atom and a chlorine atom are simultaneously transferred in opposite directions between a silylene and a silane are considered along with the insertion reactions. These proceed through the four centered transition state illustrated in Figure 2c, and have higher barriers than the insertions. Since these direct reactions would have different pressure dependence than

TABLE 7: Energetics and Rate Constants for Insertion and Exchange Reactions

reaction	TS	barrier	*k*(298)	*k*(1000)
$SiH_2 + SiH_4 \rightarrow H_3SiSiH_3$	a	−6.4		2.1E−11
$SiH_2 + SiH_4 \rightarrow H_3SiSiH_3$	d	−8.2		8.0E−11
$SiH_2 + SiH_3Cl \rightarrow H_2ClSiSiH_3$[b]	a	−5.8		4.1E−12
$SiH_2 + SiH_3Cl \rightarrow H_2ClSiSiH_3$[b]	d	−7.0		5.2E−12
$SiH_2 + SiH_3Cl \rightarrow H_2ClSiSiH_3$[c]	a	0.0		2.3E−13
$SiH_2 + SiH_3Cl \rightarrow SiHCl + SiH_4$	c	7.6		1.9E−15
$SiH_2 + SiH_2Cl_2 \rightarrow HCl_2SiSiH_3$	a	−4.8		1.5E−12
$SiH_2 + SiH_2Cl_2 \rightarrow H_2ClSiSiH_2Cl$	a	−4.0		2.3E−13
$SiH_2 + SiH_2Cl_2 \rightarrow SiHCl + SiH_3Cl$	c	5.7		1.2E−15
$SiH_2 + SiHCl_3 \rightarrow H_3SiSiCl_3$	a	−4.8		2.1E−12
$SiH_2 + SiHCl_3 \rightarrow HCl_2SiSiH_2Cl$	a	−1.5		1.5E−13
$SiH_2 + SiHCl_3 \rightarrow SiHCl + SiH_2Cl_2$	c	4.7		3.2E−15
$SiH_2 + SiCl_4 \rightarrow Cl_3SiSiH_2Cl$	a	0.7		2.1E−13
$SiH_2 + SiCl_4 \rightarrow SiHCl + SiHCl_3$	c	7.0		1.6E−15
$SiHCl + SiH_4 \rightarrow H_2ClSiSiH_3$	a	4.8	1.8E−17	2.0E−14
$SiHCl + SiH_4 \rightarrow SiH_2 + SiH_3Cl$	c	17.4	7.7E−27	2.0E−17
$SiHCl + SiH_3Cl \rightarrow H_2ClSiSiH_2Cl$	a	0.9	1.1E−15	1.9E−14
$SiHCl + SiH_3Cl \rightarrow HCl_2SiSiH_3$	a	5.1	9.6E−19	3.1E−15
$SiHCl + SiH_3Cl \rightarrow SiH_2 + SiH_2Cl_2$	c	13.1	4.7E−25	1.1E−17
$SiHCl + SiH_3Cl \rightarrow SiCl_2 + SiH_4$	c	9.5	6.1E−22	3.3E−16
$SiHCl + SiH_2Cl_2 \rightarrow HCl_2SiSiH_2Cl$[b]	a	2.4	4.1E−17	5.4E−15
$SiHCl + SiH_2Cl_2 \rightarrow HCl_2SiSiH_2Cl$[c]	a	1.9	5.2E−17	4.6E−15
$SiHCl + SiH_2Cl_2 \rightarrow SiH_2 + SiHCl_3$	c	12.0	1.3E−24	1.1E−17
$SiHCl + SiH_2Cl_2 \rightarrow SiCl_2 + SiH_3Cl$	c	6.6	1.5E−20	2.4E−16
$SiHCl + SiHCl_3 \rightarrow Cl_3SiSiH_2Cl$	a	4.2	1.6E−18	2.2E−15
$SiHCl + SiHCl_3 \rightarrow HCl_2SiSiHCl_2$	a	2.8	1.6E−17	5.0E−15
$SiHCl + SiHCl_3 \rightarrow SiH_2 + SiCl_4$	c	15.6	1.3E−27	8.6E−19
$SiHCl + SiHCl_3 \rightarrow SiCl_2 + SiH_2Cl_2$	c	7.4	1.2E−20	6.4E−16
$SiHCl + SiCl_4 \rightarrow Cl_3SiSiHCl_2$	a	5.0	1.8E−18	7.5E−15
$SiHCl + SiCl_4 \rightarrow SiCl_2 + SiHCl_3$	c	10.2	3.0E−22	4.1E−16
$SiCl_2 + SiH_4 \rightarrow HCl_2SiSiH_3$	a	20.5	3.8E−29	7.0E−18
$SiCl_2 + SiH_4 \rightarrow SiHCl + SiH_3Cl$	c	23.1	6.2E−31	2.5E−18
$SiCl_2 + SiH_3Cl \rightarrow HCl_2SiSiH_2Cl$	a	16.3	4.3E−27	8.4E−18
$SiCl_2 + SiH_3Cl \rightarrow Cl_3SiSiH_3$	a	12.6	2.1E−24	8.9E−17
$SiCl_2 + SiH_3Cl \rightarrow SiHCl + SiH_2Cl_2$	c	18.3	7.5E−29	1.4E−18
$SiCl_2 + SiH_2Cl_2 \rightarrow HCl_2SiSiHCl_2$	a	19.1	9.9E−30	7.7E−19
$SiCl_2 + SiH_2Cl_2 \rightarrow Cl_3SiSiH_2Cl$	a	10.4	2.1E−23	7.9E−17
$SiCl_2 + SiH_2Cl_2 \rightarrow SiHCl + SiHCl_3$	c	19.3	1.2E−29	1.2E−18
$SiCl_2 + SiHCl_3 \rightarrow HCl_2SiSiCl_3$[b]	a	20.6	1.1E−30	6.4E−19
$SiCl_2 + SiHCl_3 \rightarrow HCl_2SiSiCl_3$[c]	a	12.0	2.1E−24	6.3E−17
$SiCl_2 + SiHCl_3 \rightarrow SiHCl + SiCl_4$	c	23.3	8.4E−33	1.2E−19
$SiCl_2 + SiCl_4 \rightarrow Cl_3SiSiCl_3$	a	12.5	2.6E−24	1.3E−16
$H_3SiSiH + H_2 \rightarrow H_3SiSiH_3$	b	−0.5	3.2E−12	7.9E−13
$H_2ClSiSiH + H_2 \rightarrow H_2ClSiSiH_3$	b	−0.7	6.0E−12	1.4E−12
$HCl_2SiSiH + H_2 \rightarrow HCl_2SiSiH_3$	b	−0.3	1.5E−12	6.9E−13
$Cl_3SiSiH + H_2 \rightarrow Cl_3SiSiH_3$	b	−0.4	1.1E−12	3.8E−13
$H_3SiSiCl + H_2 \rightarrow H_2ClSiSiH_3$	b	9.8	7.8E−20	4.6E−15
$H_2ClSiSiCl + H_2 \rightarrow H_2ClSiSiH_2Cl$	b	10.0	6.3E−20	4.5E−15
$HCl_2SiSiCl + H_2 \rightarrow HCl_2SiSiH_2Cl$	b	9.9	3.6E−20	2.7E−15
$Cl_3SiSiCl + H_2 \rightarrow Cl_3SiSiH_2Cl$	b	10.5	6.6E−21	9.6E−16

[a] Energies are in kcal/mol. Reaction barriers are at 0 K, including zero-point energy, calculated as described in the text. TS refers to the transition-state structures of Figure 2. Estimated rate constants at 298 and 1000 K are in units of $cm^3 molecule^{-1} s^{-1}$. [b] Transition state corresponding to insertion into a Si−H bond. [c] Transition state corresponding to insertion into a Si−Cl bond.

the insertion reactions, they may play a role at high temperatures and low pressures. Figure 3 illustrates these paths along with the insertions for reactions involving trichlorinated species.

SiH_2 Insertion and Exchange Reactions. Silylene insertions into Si−H bonds are all found to have saddle points on the potential surface which lie substantially below the separated reactants, typically by about 5 kcal/mol. The energetics show very little change with substitution of chlorine on the silane into which the silylene is inserting, provided insertion is into the Si−H bond. As mentioned above, there may be paths for these reactions that are completely barrierless. These reactions should behave much like the well-studied silylene insertion into silane, which shows a small negative activation energy that becomes more negative with increasing temperature. Insertions into Si−Cl bonds have higher barriers than insertions into Si−H bonds, but the saddle points are still at or slightly below the energy of the separated reactants. The rate constants in Table 7 are calculated assuming a tight transition state at the location of the saddle point on the potential surface. This results in overestimates of the rate constants, especially at low temperatures, where the transition state should be much closer to the products, and therefore at higher energy. No room-temperature rate constants are presented for the silylene reactions because calculations using a tight transition state do not give reasonable results for many of the insertions. At 1000 K the predicted rate constant for silylene insertion into silane is in reasonable agreement with experimental results.[4] Transition states for direct exchange of a hydrogen atom for a chlorine atom to give SiHCl were located and have barriers which are 5−7 kcal/mol above the separated reactants. Due to the relatively high barriers, these paths are not expected to be observed except at very high temperatures or at low pressures, where falloff effects have reduced the rate of the insertion reactions.

SiHCl Insertion and Exchange Reactions. Barriers for insertion of SiHCl into Si−H bonds are predicted to range from 1 to 5 kcal/mol, with no clear trend with increasing chlorination of the silane into which it is inserting. Likewise, barriers for insertion of SiHCl into Si−Cl bonds range from 2 to 5 kcal/mol, again with no clear trend observed as the silane is chlorinated. However, for the three cases where there is competition between the two processes, there is a relative trend. For reaction with SiH_3Cl, insertion into the Si−H bond is faster. For reaction with SiH_2Cl_2 the rates are nearly the same. Finally, for reaction with $SiHCl_3$, insertion into the Si−Cl bond is faster. The insertion barriers are smaller than for SiHCl insertion into diatomics. Insertions of SiHCl into H_2 and HCl were predicted to have barriers of 7 and 20 kcal/mol, respectively.[15] Exothermic exchange reactions that convert SiHCl to $SiCl_2$ have barriers of 7−10 kcal/mol, lying 5−8 kcal/mol above the lowest energy insertion barrier. Again these might become competitive at high temperatures and low pressures. The endothermic exchange reactions which convert SiHCl to SiH_2 have barriers of 12−17 kcal/mol and are therefore not likely to be important.

Ho et al.[21] measured room-temperature rates of insertion of SiHCl into SiH_4 and SiH_2Cl_2. Consistent with our results, they found that the rates were roughly the same. However, our predicted rates at room temperature are nearly 2 orders of magnitude smaller than what they observed. This is not as bad a disagreement as it might first appear, since these room-temperature rates are very sensitive to the activation barrier. Lowering the barriers by about 2−3 kcal/mol would bring our estimates in line with the experimental observations. Additionally, our treatment of the low-frequency modes of the transition state as harmonic vibrations likely results in somewhat of an underestimate of the preexponential factor. Loosening of the transition structure by treating these modes anharmonically would also bring our estimates closer to the observations of Ho et al.

$SiCl_2$ Insertion and Exchange Reactions. Barriers for insertion of $SiCl_2$ into Si−H bonds range from 16 to 21 kcal/mol, while barriers for insertion into Si−Cl bonds are only 10−13 kcal/mol. We see that $SiCl_2$ preferentially reacts with Si−Cl bonds, whereas SiH_2 preferentially reacted with Si−H bonds, and SiHCl exhibited no clear preference. Consistent with previous studies, $SiCl_2$ is predicted to be much less reactive than SiH_2 or SiHCl. For comparison, the barriers for insertion into HCl and H_2 were predicted to be 16 and 40 kcal/mol, respectively.[15] The exchange reactions that convert $SiCl_2$ to SiHCl have barriers of 18−23 kcal/mol. Thus, they are consistently slower than than the insertion reactions, having barriers that are 3−11 kcal/mol higher than the lowest energy insertion channel.

Chlorinated Silylsilylene Insertions into H_2. Insertions of $H_nCl_{3-n}SiSiH$ into H_2 all have transition states that are essentially isoenergetic with the separated reactants, ranging from 0.3 to 0.7 kcal/mol below the reactants. Chlorine substitution on the tetravalent silicon is predicted to have almost no effect. Insertions of $H_nCl_{3-n}SiSiCl$ into H_2 have barriers near 10 kcal/mol. Again, chlorine substitution on the tetravalent silicon has almost no effect. However, chlorine substitution on the divalent silicon raises the insertion barrier by 10 kcal/mol. This is a smaller effect than is seen for chlorine substitution on silylene. SiH_2, SiHCl, and $SiCl_2$ have insertion barriers for reaction with hydrogen of 2, 20, and 40 kcal/mol, respectively. Thus, chlorine substitution on the divalent silicon of the silylsilylenes raises the insertion barrier only about half as much as is observed for chlorine substitution on the silylenes.

Summary and Conclusions

The thermochemistry and reaction kinetics of the thermal decomposition of the chlorinated disilanes have been explored using high-level ab initio calculations. These results provide a basis for the modeling of multistep homogeneous decomposition of chlorinated silanes and a basis for predicting the reactivity of the compounds considered. Comparable energy barriers were found for the different possible elimination reactions, with different reactions dominating for different chlorinated disilanes. In addition to the insertion reactions, which are the reverse of the thermal decomposition reactions, new reaction paths were found where a hydrogen and chlorine atom are simultaneously exchanged between a chlorinated silane and a chlorinated silylene in a concerted four-centered process. These paths may become important at high temperatures and low pressures, where the insertion reactions exhibit falloff effects.

Acknowledgment. M.T.S. would like to thank the National Science Foundation and the University of Minnesota for support in the form of graduate fellowships. Generous grants of supercomputer time from the Minnesota Supercomputer Institute were used for portions of these calculations and are gratefully acknowledged.

References and Notes

(1) Gordon, M. S.: Francisco, J. S.; Schlegel, H. B. *Adv. Silicon Chem.* **1993**, *2*, 137.

(2) Becerra, R.: Walsh, R. In *Research in Chemical Kinetics*, Compton, R. G.; Hancock, G., Eds.; Elsevier Science: Amsterdam, 1995; Vol. 3.

(3) Jasinski, J. M.; Becerra, R.; Walsh, R. *Chem. Rev.* **1995**, *95*, 1203.

(4) Becerra, R.; Frey, H. M.; Mason, B. P.; Walsh, R.; Gordon, M. S. *J. Chem. Soc., Faraday Trans.* **1995**, *91*, 2723.

(5) Becerra, R.; Frey, H. M.; Mason, B. P.; Walsh, R.; Gordon, M. S. *J. Am. Chem. Soc.* **1992**, *114*, 2751.

(6) Inoue, G.; Suzuki, M. *Chem. Phys. Lett.* **1985**, *122*, 361.

(7) Jasinski, J. M.; Chu, J. O. *J. Chem. Phys.* **1988**, *88*, 1678.

(8) Baggot, J. E.; Frey, H. M.; Lightfoot, P. D.; Walsh, R.; Watts, I. M. *J. Chem. Soc., Faraday Trans.* **1990**, *86*, 27.

(9) Martin, J. G.; Ring, M. A.; O'Neal, H. E. *Int. J. Chem. Kinet.* **1987**, *19*, 715.

(10) Gordon, M. S.; Gano, D. R. *J. Am. Chem. Soc.* **1984**, *106*, 5421.

(11) Gordon, M. S.; Truong, T. N.; Benderson, E. K. *J. Am. Chem. Soc.* **1986**, *108*, 2191.

(12) Sakai, S.; Nakamura, M. *J. Phys. Chem.* **1993**, *97*, 4960.

(13) Trinquier, G. *J. Chem. Soc., Faraday Trans.* **1993**, *89*, 775.

(14) Su, M.-D.; Schlegel, H. B. *J. Phys. Chem.* **1993**, *97*, 8732.

(15) Su, M.-D.; Schlegel, H. B. *J. Phys. Chem.* **1993**, *97*, 9981.

(16) Wittbrodt, J. M.; Schlegel, H. B. *Chem. Phys. Lett.* **1997**, *265*, 527.

(17) Hay, J. P. *J. Phys. Chem.* **1996**, *100*, 5.

(18) Ignacio, E. W.; Schlegel, H. B. *J. Phys. Chem.* **1992**, *96*, 1758.

(19) McKean, D. C.; Palmer, M. H.; Guest, M. F. *J. Mol. Struct.* **1996**, *376*, 289.

(20) McKean, D. C.; McPhail, A. L.; Edwards, H. G. M.; Lewis, I. R.; Mastryukov, V. S.; Boggs, J. E. *Spectrochim. Acta* **1993**, *49A*, 1079.

(21) Ho, P.; Breiland, W. G.; Carr, R. W. *Chem. Phys. Lett.* **1986**, *132*, 422.

(22) Jenkins, R. L.; Vanderwielen, A. J.; Ruis, S. P.; Gird, S. R.; Ring, M. A. *Inorg. Chem.* **1973**, *12*, 2968.

(23) Doncaster, A. M.; Walsh, R. *J. Chem. Soc., Faraday Trans. 1* **1980**, *76*, 272.

(24) Frisch, M. J.; Trucks, G. W.; Schlegel, H. B.; Gill, P. M. W.; Johnson, B. G.; Robb, M. A.; Cheeseman, J. R.; Keith, T.; Petersson, G. A.; Montgomery, J. A.; Raghavachari, K.; Al-Laham, M. A.; Zakrzewski, V. G.; Ortiz, J. V.; Foresman, J. B.; Cioslowski, J.; Stefanov, B. B.; Nanayakkara, A.; Challacombe, M.; Peng, C. Y.; Ayala, P. Y.; Chen, W.; Wong, M. W.; Andres, J. L.; Replogle, E. S.; Gomperts, R.; Martin, R. L.; Fox, D. J.; Binkley, J. S.; Defrees, D. J.; Baker, J.; Stewart, J. P.; Head-Gordon, M.; Gonzalez, C.; Pople, J. A. *GAUSSIAN 94*, revision D.2; Gaussian, Inc.: Pittsburgh, PA, 1995.

(25) Curtiss, L. A.; Raghavachari, K.; Pople, J. A. *J. Chem. Phys.* **1993**, *98*, 1293.

(26) Curtiss, L. A.; Raghavachari, K.; Trucks, G. W.; Pople, J. A. *J. Chem. Phys.* **1991**, *94*, 7221.

(27) Pople, J. A.; Head-Gordon, M. H.; Raghavachari, K. *J. Chem. Phys.* **1987**, *87*, 5968.

(28) Curtiss, L. A.; Raghavachari, K.; Deutsch, P. W.; Pople, J. A. *J. Chem. Phys.* **1991**, *95*, 2433.

(29) Bethke, G. W.; Wilson, K. W. *J. Chem. Phys.* **1957**, *26*, 1107.

(30) Chase, M. W.; Davies, C. A.; Downey, J. R.; Frurip, D. J.; McDonald, R. A.; Szverud, A. N. *JANAF Thermochemical Tables*, 3rd. ed.; *J. Phys. Chem. Ref. Data* **1985**, 14.

(31) Pedley, J. B.; Iseard, B. S. *CATCH Tables for Silicon Compounds*; University of Sussex, 1972.

(32) Steinfeld, J. I.; Francisco, J. S.; Hase, W. L. *Chemical Kinetics and Dynamics*; Prentice Hall: Englewood Cliffs, NJ, 1989.

(33) Dzarnoski, J.; Rickborn, S. F.; O'Neal, H. E.; Ring, M. A. *Organometallics* **1982**, *1*, 1217.

(34) Ring, M. A.; O'Neal, H. E. *J. Phys. Chem.* **1992**, *96*, 10848.